An optimised 3 M KCl salt-bridge technique used to measure and validate theoretical liquid junction potential values in patch-clamping and electrophysiology

Peter H. Barry • Trevor M. Lewis • Andrew J. Moorhouse

Published online (21 June 2013) in the *European Biophysics Journal*
DOI: 10.1007/s00249-013-0911-3

Abstract: Accurate potential measurements in electrophysiological experiments require correction for liquid junction potentials (LJPs), and in patch-clamping especially these can often be ~5-10 mV or more. They can be either calculated, if ion mobilities are known, or measured directly. We describe an optimised system to directly measure LJPs with a patch-clamp amplifier, using as a reference electrode, a freshly-cut 3 M KCl-agar salt-bridge (in polyethylene tubing) with its tip cut off by at least 5 mm during solution changes to eliminate its solution-history-dependent effects. We quantify such history-dependent effects and complement this with a *de-novo* theoretical analysis of salt diffusion to and from the salt-bridge. Our analysis and experimental results validate the optimised methodology for measuring LJPs, and the use of the Henderson equation for accurately calculating them. The use of this equation is also assessed and generally validated in the light of rigorous Nernst-Planck-Poisson and other numerical simulation and analytical studies of LJPs over recent decades. Digitizing, recording and amplifying the measured potentials increases their accuracy. The measured potentials still need correction for small, well-defined calculable, shifts in LJPs at the 3 M KCl-agar reference. Using this technique, we have measured changes in LJPs for diluted solutions of NaCl, LiCl, KCl, CsCl and NaF, obtaining excellent agreement within ± 0.1 mV of predicted values, calculated using ion activities. Our *de novo* LJP measurements of biionic combinations of the above undiluted salts, and NaI and NaF (with halide anions I^- and F^-), generally also gave excellent agreement with predicted values.

Keywords: Liquid junction potentials · Patch-clamp · Reference electrodes · Salt-bridges · 3 M KCl · Ion activities

P.H. Barry, T.M. Lewis, A.J. Moorhouse, Department of Physiology, School of Medical Sciences, University of New South Wales, Sydney, UNSW, NSW 2052, Australia.
Corresponding Author: Peter H. Barry, Tel.: +61-2-9385 1101; Email: p.barry@unsw.edu.au

Electronic Supplementary Material is appended at the end of this article.

Introduction

Accurate membrane potential and other potential measurements in electrophysiological experiments require careful corrections for liquid junction potentials (LJPs). The LJPs arise at the interface of two solutions of different ionic composition, as the cations and anions, with different mobilities, diffuse down the respective concentration (and electrical) gradients of each ion. This results in charge separation and the development of the potential difference between the two solutions. In patch-clamp experiments especially, where the pipette solution often contains anions and cations of very different mobilities (e.g., K_2SO_4 or TEACl), these LJPs can be as large as ~10 mV or more at physiological concentrations. Similarly, when measurements are made between two solutions of very different ionic strength, as occurs in dilution potential experiments used to determine relative ion permeabilities, the shifts in LJP can be very large (e.g., ~10 mV for a 25% dilution of LiCl). The problem has been appreciated for some time, and is described in a topical review by Barry and Lynch (1991), where it is clearly shown that these LJPs are not eliminated (as is sometimes erroneously assumed) by the procedure for zeroing the electrode offset prior to patching a cell. Two approaches are used to accurately determine the values of these LJPs: to calculate them theoretically or to experimentally measure them. Where the ion mobilities are known, theoretical calculations can be more readily done (Barry 1994), and commercial software is also available to do this with the Windows version of the *JPCalc* program (now in pCLAMP software from Molecular Devices Corp, or as a stand-alone program *JPCalcW* from SDR Scientific, Sydney). In order to validate such theoretical calculations, or if ion mobilities are not well known, it is necessary to measure the LJPs experimentally. Procedures for direct experimental LJP measurements have been described (e.g., Neher 1992, 1995), but these still require a correction for the change in LJP at the reference electrode interface with the bath solution. Ideally then, such direct measurements require a reference electrode that either has a potential with a known dependence on the activities of one of the ions in the bath solution (e.g., Cl^- with an Ag/AgCl electrode) that can be calculated, or has a potential that is independent of changes in bath solution composition. In the former case, the reference corrections can be large, reliant on high quality Ag/AgCl electrodes and dependent on no significant electrode potential contributions from other competing ions. In the latter case, a 3 M KCl

reference electrode can, in principle, have a minimal dependence on changes in bath solution composition, because its LJP is dominated by the high concentration of K^+ and Cl^- ions with similar, but not equal, mobilities. These 3 M KCl electrodes may be free-flowing microelectrodes (or patch-pipettes) or agar salt-bridges. Free-flowing microelectrodes can easily become non-free flowing, due to surface tension effects at the microelectrode shaft or blockage at the tip. In addition, it is possible that free-flowing pipettes may result in convective flow effects that may affect LJPs (see Discussion). Free-flowing 3 M KCl patch-clamp pipettes also have the potential to result in KCl contamination of the test solutions. Furthermore, a 3 M KCl electrode in combination with a 150 mM NaCl salt bridge would have an Ag/AgCl offset potential of about 70 mV, which would need to remain stable within about 0.1 mV during the measurements to achieve accurate results. The 3 M KCl-agar salt-bridge would seem to be a very straightforward alternative, were it not for its notorious history-dependent behaviour due to contamination of the tip by the various test solutions into which it is placed (identified and discussed in Barry and Diamond 1970, and Neher 1992). However, these history-dependent changes in LJP and instability can be overcome by simply cutting off the end of the 3 M KCl agar salt-bridge (in polyethylene tubing) just before each solution transfer (e.g., Barry et al. 2010; Sugiharto et al. 2010). The LJP correction for a fresh 3 M KCl salt-bridge, small but not insignificant, can be calculated and applied in the appropriate direction to result in the precise determination of LJPs.

This present article describes an optimised "freshly-cut 3 M KCl salt-bridge" methodology and directly quantifies the history-dependent effects with a de-novo theoretical analysis. Our analysis and experimental results validate the optimised methodology for measuring LJPs, and the use of the Henderson equation with its high degree of accuracy for calculating them. The validity of using this equation for calculating pseudo 'steady-state' LJPs is also assessed and justified in the light of rigorous Nernst-Planck-Poisson and other numerical simulation and analytical studies of LJPs over recent decades (summarised just before the Discussion section and given in full in the online Electronic supplementary material, referred to as **ESM**). Using our optimised approach we measured LJPs with greater accuracy for diluted solutions of NaCl, LiCl, KCl and CsCl and made new LJP measurements of NaF dilutions and biionic combinations of all the undiluted salts. We show that these re-measured values (corrected for the 3 M KCl LJPs) for the dilution potentials give excellent agreement, within the small experimental errors of ±0.1 mV, with LJPs theoretically calculated using the Henderson equation and ion activities (with *JPCalcW*). Similarly, there is generally excellent agreement between measured and predicted LJPs in biionic situations. We also measured LJPs for non-chloride solutions with two other halides, fluoride and iodide with relative mobilities at the low and high end range of the halides. Again, there was generally excellent agreement between measured and predicted LJPs in biionic and dilution situations.

The theoretical analysis of the history-dependent behaviour of these 3 M KCl-agar salt-bridges involves solving the equations for diffusion of test solute from a solution bath into the 3 M KCl salt-bridge, and diffusion of the KCl from the salt-bridge into the solution bath. We now present these mathematical solutions, which we show justifies our experimental LJP measurement methodology and quantitatively supports the length of the salt-bridge that is cut off.

Methods and materials

Solutions

In order to mimic typical simplified electrophysiological extracellular solutions, the NaCl, KCl, LiCl and CsCl solutions contained a pH buffer (HEPES) titrated to pH 7.4 with the appropriate hydroxide (NaOH, KOH, LiOH or CsOH) and some glucose. Sucrose was added to the diluted solutions to maintain osmolality. For example, for the NaCl dilution data (Sugiharto et al. 2010), the "1.0" NaCl solution consisted of 145 mM NaCl, 10 mM glucose plus 10 mM HEPES titrated to pH 7.4 with ~5 mM NaOH to give approximate ionic concentrations in mM of Na^+, Cl^- and $HEPES^-$ of 150, 145 and 5 respectively. The 0.5 NaCl solution differs from this 1.0 NaCl solution in that it has 75 mM NaCl, plus an added 136 mM sucrose, to give approximate ionic concentrations (in mM) of Na^+, Cl^- and $HEPES^-$ of 80, 75 and 5 respectively. The 0.25 NaCl solution has 37.5 mM NaCl and 189 mM sucrose, and has approximate ionic concentrations in mM of Na^+, Cl^- and $HEPES^-$ of 42.5, 37.5 and ~5 respectively. The biionic solutions were the non-diluted 1.0 XCl solutions. For full details of the NaCl, KCl, LiCl and CsCl solutions used in this article and the purity and source of the salts, see **ESM**.

Ion activities

The calculations of activities for each of the ions in any solution, were determined by initially evaluating the total ionic strength, I, of the solution to account for all monovalent and any divalent ions in the solution, and then determining the activity coefficient of the predominant salt in solution from numerical fits to published NaCl, KCl, LiCl and CsCl solutions, and then applying this to each of the ions. This is outlined in the **ESM**, together with examples of activity calculations in Table S1.

Experimental setup and basic principles

The basic experimental setup is shown in Fig. 1. It consists of two electrode-salt-bridge combinations, with the salt-bridges dipping into one of two (control and test) solution beakers (light yellow). The control solution is 1.0 XCl solution, where X represents the predominant cation (Na^+, K^+, Li^+ or Cs^+) in the solution, and the test solution is either, the 0.5 XCl or 0.25 XCl, for dilution measurements, or 1.0 YCl solution, where Y is a different cation from the X for biionic measurements (or NaZ, where Z is I or F for the anion in biionic measurements). The left electrode 150 mM XCl salt-bridge is allowed to initially equilibrate with the control solution, so that the composition at the end of the 150 mM XCl salt-bridge

becomes very similar to that of the control solution (1.0 XCl) for the LJP measurements. At each salt-bridge the LJP is defined as solution – salt-bridge, and as indicated in the figure, the true shift in LJP (ΔV_{LJ}^{m}) at the XCl salt-bridge, defined as test solution – control, is related to the shift in amplifier potential ΔV_{exp} and the shift in the LJP correction at the freshly-cut 3 M KCl salt-bridge ΔV_{3M} by:

$$\Delta V_{LJ}^{m} = -\Delta V_{exp} + \Delta V_{3M} \qquad (1)$$

The same basic setup was used for control solutions with a predominant anion different from Cl (e.g., XA, where A represents that anion), with the left salt-bridge replaced by a 150 mM XA salt-bridge, but with both the left salt-bridge electrode and conical flask still containing 150 mM XCl).

The Ag/AgCl electrodes were encased in truncated glass Pasteur pipettes filled with simple 150 mM XCl solutions gelled with 4% agar (w/v; 4g/100 ml) and sealed at the air-Ag/AgCl-salt interface by a silicon compound (Sylgard 184, Dow Corning) to minimize electrode deterioration (see **ESM**). We used an Axopatch 200B patch-clamp amplifier and Digidata 1440A (Molecular Devices Corp., Sunnyvale, CA, USA) with gap-free acquisition at 1 kHz and 200 Hz low-pass filter for all but the later measurements with NaI and NaF solutions. For these later measurements an Axopatch-ID patch-clamp amplifier was used with acquisition at 500 Hz and 100 Hz low-pass filter. The Axopatch-1D traces were also digitally filtered after recording with a 50 Hz low-pass Gaussian filter (E.g., Fig. 4) to further reduce the increased noise with this amplifier. During measurement of LJPs, the amplifier voltage was digitized and recorded using the Clampex program in pCLAMP 10 software, which increased the precision of the measurements over that of the digital readout display (± 0.1 mV for the Axopatch 200B amplifier and ± 1 mV for the Axopatch-ID amplifier). Alternatively, instead of a patch-clamp amplifier, a very high input impedance electrometer could be used. The salt-bridges constructed of polyethylene tubing (ID 2.0 mm, OD 3.0 mm) were filled with either 150 mM XCl or 3 M KCl gelled with 4% (w/v) agar. For further details see **ESM**.

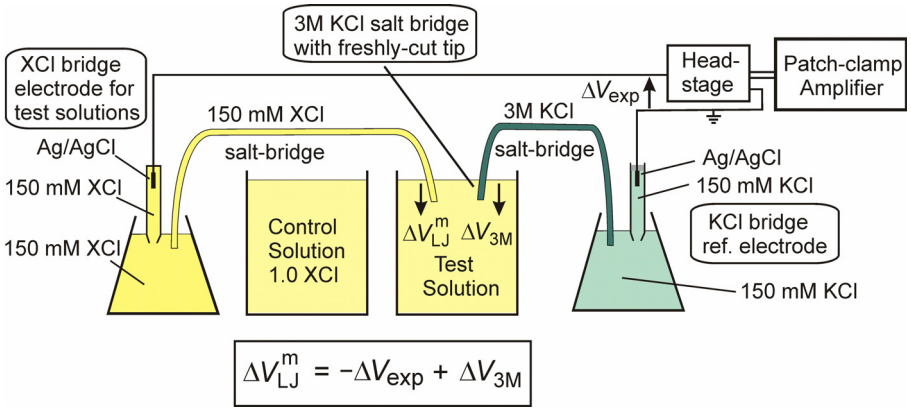

Fig. 1. The experimental set up for directly measuring the shift in LJP (ΔV_{LJ}^{m}) between test and control 1.0 XCl solutions at a 150 mM XCl salt-bridge, with its tip equilibrated to 1.0 XCl, where X represents the predominant cation (e.g., Li^+, Na^+, K^+ or Cs^+). Initially both salt-bridges are placed in the left 1.0 XCl control solution beaker and allowed to equilibrate for some time to enable the tip of the XCl salt-bridge to have a composition of 1.0 XCl (with 145 mM XCl, 10 mM HEPES, 5 mM glucose and about 4 mM XOH, with pH 7.4) and to let whole system stabilize (see text). Then the beaker is replaced with fresh 1.0 XCl solution, which is used for the rest of the set of measurements. After this long equilibration, the end of the 3 M KCl salt-bridge is cut off by about 2-3 cm, but thereafter it is cut-off by at least 5 mm, each time it is transferred between solutions. The ends of both salt-bridges are also carefully wiped with tissue during each solution transfer. Typically, the two salt-bridges are then sequentially transferred to a test solution, which either contains a diluted XCl (e.g., 0.5 XCl or 0.25 XCl) for the dilution experiments or a 1.0 YCl solution for biionic experiments for about a minute, where Y refers to the same set of cations but different from X, and then returned to the control 1.0 XCl solution for 2-3 min. The salt-bridges are gelled in 4% (w/v) agar and enclosed in polyethylene tubing. The electrode potentials are measured either by connection to the head-stage of a patch-clamp amplifier (as for the data in this article) or to a high-impedance electrometer. $\Delta V_{3\,M}$ and ΔV_{exp} refer to the shift in the LJP at the 3 M KCl salt-bridge and the experimental recorded shift in amplifier voltage. In each case, these potential shifts refer to the test value – control value, and the equation in the figure inset relates ΔV_{LJ}^{m} to ΔV_{exp} and ΔV_{3M} (Eq. 1 in text). This is a modified version of Fig. 3 of Barry et al. (2010).

Experimental protocol

Initially, the whole circuit was connected up as in Fig. 1, but with both salt-bridges in the control (1.0 XCl) solution beaker, using the voltage-clamp mode of the amplifier, with the voltage display zeroed by adjusting the amplifier pipette offset. Since the pure 150 mM XCl salt-bridge differs slightly from the actual 1.0 XCl physiological control solution, it should initially be left to equilibrate in the 1.0 XCl solution for at least 30 mins, to allow its tip to be replaced by XCl control solution and to behave as a 1.0 XCl salt-bridge throughout the rest of the experiment. In practice, the whole circuit was left connected up for about 2 hours to also allow the Ag/AgCl electrodes to stabilize, after which 20-30 mm was cut off the end of the 3 M KCl salt-bridge and the control solution replaced for the rest of the measurements. (N.B. *The same procedure was used for non-Cl 1.0 XA control solutions, where A represents a different anion than Cl).*

For example, for a 0.5 dilution experiment, the normal procedure was as follows: Let the salt-bridges equilibrate as above and zero the amplifier voltage. Start voltage recording. After a few minutes in the 1.0 XCl control solution, the two salt-bridges were then transferred into a beaker with the 0.5 XCl test solution, where they were left

for about 1 minute, after which they were transferred back into the beaker with the 1.0 XCl control solution for a few minutes. During each transfer of the salt-bridges between beakers the tip of the 3 M KCl agar-salt-bridge was cut off by at least 5 mm, before being placed into the new beaker, to ensure the salt-bridge tip is composed of fresh 3 M KCl. In addition, to minimize any solution contamination between beakers, the end 10 cm or so of both salt-bridges are wiped dry with tissue before they are transferred into the new beaker. The same procedure was used for XCl to YCl biionic potential measurements (and for XCl to XA, or XA to XB, where both A and B are different from Cl and from each other). Typical segment records of LJP measurements can be seen later in Figs. 3 and 4 (and Figs S2-S5 in the **ESM**).

be so readily expressed as mixtures of the end solutions, so that the LJP may not be quite so well defined and stable (see comments with Eqs. 2 and 3 following).

Correction for the 3 M KCl salt-bridge LJP

While ΔV_{3M} is relatively small, it is generally significant. For example, 0.5 and 0.25 dilutions of LiCl resulted in ΔV_{3M} values of -0.7 and -1.3 mV respectively (Table 2), calculated using ion activities with the program *JPCalcW* (Windows version; cp. Barry 1994). Using ion concentrations in the calculations only very rarely changed these values, due to rounding errors (see Table 2 for a 0.25 dilution of NaCl). An example of the use of the

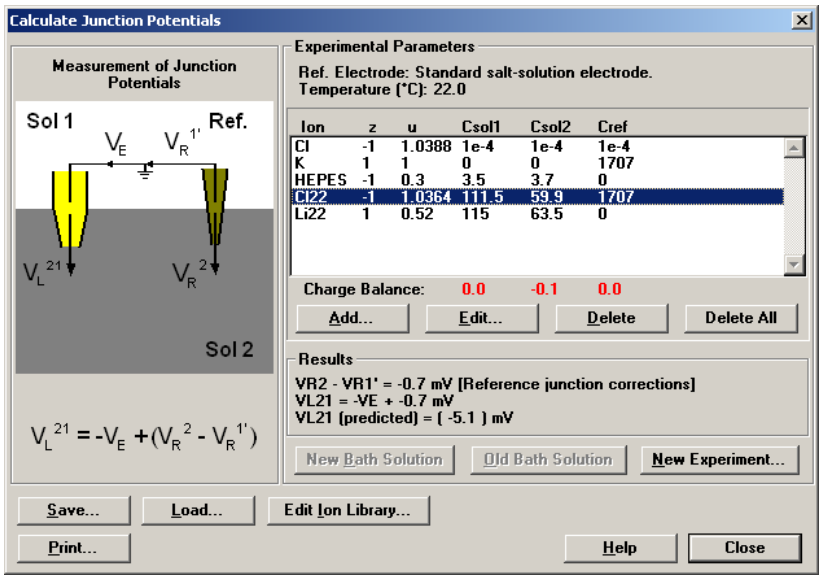

Fig. 2. An example of the use of the *JPCalc for Windows* program in determining the 3 M KCl reference LJP (ΔV_{3M}) needed in the correction of the measured shift (ΔV_{exp}) in LJPs to obtain the corrected measured LJP. The example shown is for a 0.5 LiCl dilution (145 mM : 75 mM) experiment (as shown for LiCl in Table 2). Cl22 and Li22 refer to Cl^- and Li^+ ions, respectively, with mobilities given at 22 °C (Table 1). A trace amount of Cl^- with a 25 °C mobility from the built-in ion mobility library has been added, to reassure the program that Ag/AgCl electrodes are in contact with Cl^- ions. The experimentally measured potential, $-\Delta V_{exp} = -V_E$, in the JPCalc terminology = –4.4 mV (Table 2). The calculation of the correction for the 3 M KCl reference junction potential is shown (ΔV_{3M} = VR2 – VR1′ = –0.7 mV). The corrected measured value of VL21 = –4.4 + –0.7 = –5.1 mV (with the estimated error being about 0.1 mV) and the predicted value of the LJP shift = VL21 = –5.1 mV. Note that all ion concentrations have been converted to activities for these calculations, using activity coefficients as in Table S1 (of the **ESM**), and that 1707 mM is the activity of 3 M KCl.

It should be noted that after it has equilibrated in control solution, the right end of the 150 mM XCl or XA salt-bridge (yellow salt-bridge in Fig. 1) should not be cut off. This is because the LJP values are to be determined at this saline salt bridge and the end of the salt-bridge should have the same composition as the control solution. Furthermore, it is generally preferable to have longer salt-bridge durations in control solution than in test solution. An example of how this can affect LJP records is shown for a CsCl:LiCl biionic experiment in Fig. S6 (ESM), where for this pair of cations with very different mobilities, increasing the ratio of control/test durations from 1 to 3 times reduced a very small transient component in the voltage shift between solutions. This is not unreasonable, since if the time spent in the control solution is not much longer than in the test solution, then the tip of the XCl salt-bridge would not have re-equilibrated to the control solution composition and the composition of the layers of the solution junction may not

JPCalc program in calculating ΔV_{3M} for the 50% dilution of LiCl is shown in Fig. 2. The 3 M KCl correction and the calculated (predicted) LJP by the program were both given to the nearest 0.1 mV, so that each value has a rounding error of ± 0.05 mV. Note that the program calculates both the value of ΔV_{3M} (≡ VR2-VR1′) and the predicted LJP shift ΔV_{LJ}^{p} (≡ VL21; predicted) and indicates how the correction is applied, as indicated in Fig. 2.

LJP calculations

The *JPCalcW* program uses the generalized Henderson equation for all the LJP calculations. The activity form of the equation (Barry and Lynch 1991; cp. original concentration formulation MacInnes, 1961, P. 232) is given by:

$$V^S - V^P = (RT/F) \quad S_F \quad \ln\{\sum_{i=1}^{N} z_i^2 u_i a_i^P / \sum_{i=1}^{N} z_i^2 u_i a_i^S\} \quad (2)$$

where V^S and V^P refer to the potentials of the solution bath and the pipette solution respectively, and the summation factor, S_F, proportional to the summed contribution of the product of the activity difference across the junction and mobility for each of the cations, minus the equivalent summed contribution for each of the anions, is given by:

$$S_F = \sum_{i=1}^{N} [z_i u_i (a_i^S - a_i^P)] \quad / \quad \sum_{i=1}^{N} [z_i^2 u_i (a_i^S - a_i^P)] \qquad (3)$$

R, T and F refer to gas constant, temperature in K and Faraday's constant; and z_i, u_i, a_i refer to valency, mobility and activity of ion i, with N being the total number of ion species in all solutions; and again the superscripts refer to solution and pipette respectively.

The derivation of the equation does not require any particular arrangement of the layers of solution in the junction, only that the solutions composing the junction region should be a series of mixtures of the end solutions S and P (MacInnes 1961; P. 232). It is therefore a very versatile equation and in a later separate section the its use for calculating pseudo 'steady-state' LJPs is assessed and generally validated in the light of recent rigorous Nernst-Planck-Poisson and other numerical simulation and analytical studies of LJPs.

Table 1. Relative mobilities (u_X/u_K) of Li^+, Na^+, Cs^+, Cl^-, F^- and I^- relative to K^+, at different temperatures.

Ion (X) Temp °C	Li^+	Na^+	K^+	Cs^+	Cl^-	F^-	I^-
20	0.516	0.674	1.000	1.053	1.035	-	-
21	0.518	0.675	1.000	1.052	1.036	-	-
22	0.520	0.677	1.000	1.049	1.036	0.748	1.040
25	0.525	0.682	1.000	1.050	1.039	0.754	1.046

Values at 20, 21 and 22 °C were obtained by interpolating limiting equivalent conductance data at 15, 18, 25 and 35 °C (From Robinson and Stokes, 1965 and Dean, 1999) for the first 5 ions with a quadratic polynomial fit, and by simple linear interpolation between 18 and 25 °C data for F^- and I^-. Relative mobilities were then determined using Eq. S16 in the accompanying **ESM**.

In order to most accurately determine the 3 M KCl LJP correction and the calculated LJPs (especially for the LiCl and NaCl dilutions), it was necessary to determine the relative mobilities, u_{Li}/u_K, u_{Na}/u_K and u_{Cl}/u_K at 22 °C, the temperature at which the experiments were performed, rather than the standard values at 25 °C. Relative mobilities of all the major cations and anions were determined at this temperature (Table 1).

Electronic Supplementary Material (ESM)

The online file of electronic Supplementary material (**ESM**) provides additional information about the solutions, preparation of the Ag/AgCl electrodes, details of the calculations of ion activities of each of the salts, added sample chart records of LJP measurements (in the absence and presence of the 3 M KCl salt-bridge being cut) and a table of limiting equivalent conductivity of the ions as a function of temperature. It discusses a possible effect of electric field on Cs^+ mobility. It has more information on the concentration profile calculations in the 3 M KCl salt-bridge, a table of values and an additional expanded graph of concentration profiles after 20 min. It also includes appendices relating generalized relative ionic mobility to limiting equivalent conductivity, expanding on the validity of LJP calculations, and on practical LJP measurements.

Results

Using the Axopatch patch-clamp amplifier, shifts in LJPs were measured with a fresh 3 M KCl reference salt-bridge in which the tip was cut off each time the salt-bridge was transferred into a new solution, as described in the Methods. This was done for a number of common salts (NaCl, LiCl, KCl, CsCl, NaF and NaI), under dilution and/or biionic conditions, in order that the experimentally measured LJPs could be compared with the theoretically calculated values.

The necessity of a fresh 3 M KCl salt-bridge interface for LJP measurements

History-dependent problems due to contamination of the end of the 3 M KCl-agar reference salt-bridge are well demonstrated by the KCl:LiCl experiment in Fig. 3A. Both the 150 mM KCl and the 3 M KCl salt-bridges had initially equilibrated in the control 1.0 KCl solution for about 2 hours. On transfer to 1.0 LiCl (test) and back to 1.0 KCl (control) solutions, the slow transient responses observed (left panel of Fig. 3A) were smaller in magnitude compared to the rapid responses seen when the end of the 3 M KCl salt-bridge was cut off straight after the equilibration by about 2 cm, and then subsequently by ~8 mm upon each transfer of that salt-bridge between solutions (right panel of Fig. 3A; cf. also Figs S2-S5 in the **ESM**). Fig. S2B in the ESM shows another KCl:LiCl bionic experiment, in which even a duration of ~6 min in control KCl solution is enough to produce a transient response and a reduced magnitude in the potential shift. Subsequent transfers to 1.0 LiCl solution and back with cut 3 M KCl salt-bridges (cut by at least 6 mm) result in almost immediate rectangular shifts in potential. Fig. S3 shows that for longer conditioning durations, such as 120 min in NaCl solution, cuts of over 20 mm were needed to ensure accurate salt-bridge potentials, as will be discussed later.

Dilution liquid junction potential measurements

Figure 3B shows typical rapid potential changes (ΔV_{exp}) measured upon 0.25 dilutions of 1.0 LiCl, NaCl and CsCl when measured with a freshly-cut 3 M KCl salt-bridge (another example showing consistent rectangular shifts for a series of 0.5 and 0.25 dilutions of NaCl is given in Fig. S4 in the **ESM**).

The mean data for LJP measurements upon 0.5 and 0.25 dilutions for NaCl, LiCl, KCl, CsCl and NaF are shown in

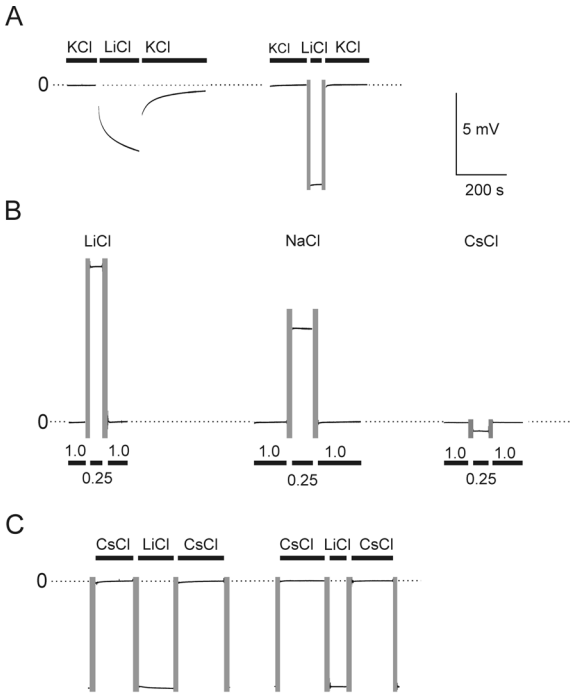

Fig. 3. Sample traces of measured liquid junction potential (LJP) shifts during bracketed solution changes measured using a 3 M KCl-agar salt-bridge reference with the experimental setup given in Fig. 1. None of these LJP shifts (ΔV_{exp}) are corrected for the LJP shift (ΔV_{3M}) at the 3 M KCl-agar salt-bridge (see Eq. 1). The vertical grey bars represent the change-over period between control and test solutions when the tip of the 3 M KCl-agar salt-bridge is cut off by at least 5 mm (in all traces except the left one in Panel A). Panel A demonstrates the necessity of cutting off the tip of the 3 M KCl salt-bridge during KCl-LiCl biionic solution changes. In the left trace, the the 3 M salt-bridge is not cut after the salt-bridges had been left in control KCl solution for 2 hrs, and on transferring both salt-bridges to LiCl solution and then back to KCl results in a slow transient responses. In the right trace (same experiment) after the 3 M KCl salt-bridge had initially been cut off by 20 mm and then by about 8 mm before each solution change, there is a clear rectangular response without significant transients, with its amplitude being close to the value predicted theoretically (Table 3). Panel B shows sample LJP responses from 1.0 to 0.25 XCl dilutions for LiCl, NaCl and CsCl solutions. Average LJP values for these solutions with all corrections and predicted values are given in Table 2. Panel C shows two trace segments from the same CsCl-LiCl biionic experiment. In the left trace, the duration in control CsCl solution is similar to that in the test LiCl solution, and with Cs^+ and Li^+ having very different mobilities, there is a slight transient response in the test solution (more clearly seen in Fig S6 in the ESM; see Discussion). In contrast, in the right trace, the duration in test solution is much less than in the control solution and the response has virtually no transient component (see also Fig. S6 in the **ESM**).

Table 2. To illustrate the contribution of the 3 M KCl reference LJP (ΔV_{3M}^{a}), the table lists the uncorrected LJP measurement ($-\Delta V_{exp}$) obtained using Eq. 1. The contribution of the 3 M KCl reference LJP (ΔV_{3M}) could be quite substantial (e.g., 0.6 mV in 2.7 mV, a 22% contribution, for the 0.5 NaCl dilution).

The corrections were done, for comparison, using both ion activities and concentrations for the 3 M KCl LJPs and the values obtained generally differed by less than 0.1 mV. The measured LJP ΔV_{LJ}^{ma} (corrected for the ΔV_{3M} LJP using activities) in every case agreed within the expected error of ± 0.1 mV, with the *JPCalcW* value predicted using ion activities and the Henderson equation (ΔV_{LJ}^{pa}). However, if ion concentrations were used, the predicted LJP values (ΔV_{LJ}^{pc}) overestimated the measured values (by up to 0.5 mV), as would be (qualitatively) expected from theoretical considerations. It should be noted that the use of the relative mobilities at 22 °C rather than 25 °C reduced the ΔV_{3M}^{a} value by 0.1 mV and increased the ΔV_{LJ}^{pa} by 0.1 mV for the 0.25 LiCl dilution.

Biionic liquid junction potential measurements

The biionic solutions used were 1.0 solution combinations of NaCl, KCl, LiCl, CsCl, NaI and NaF. The last two solutions were chosen to examine and compare biionic LJPs of halides other than Cl^-, since I^- and F^- are halides with the largest and smallest ion mobilities of the group respectively, and their properties (e.g., activity coefficients) are well known. Fig. 3C show two brief segments of the same CsCl:LiCl experiment. A longer sample KCl:NaCl experiment is shown in Fig. S5 (**ESM**). The biionic results are summarized in Table 3. As with the dilution potentials, there was excellent agreement between corrected measured LJP values and theoretically predicted values for NaCl, KCl, LiCl and NaCl:NaI and NaCl:NaF combinations, all being within experimental and predicted errors. However, for the LiCl:CsCl, NaCl:CsCl and KCl:CsCl biionic potentials, the predicted LJP values were consistently 0.2-0.3 mV more negative than the corrected measured values, somewhat beyond the ±0.1 mV resolution rounding error in the calculations (see

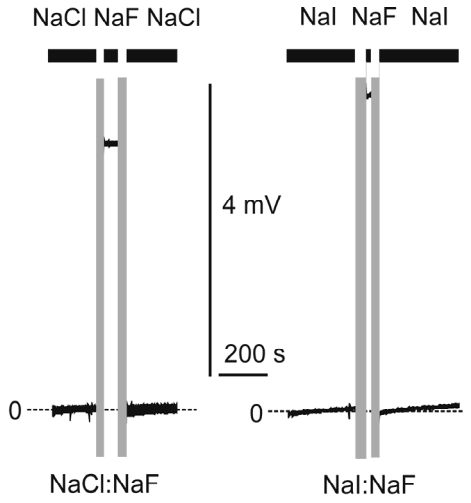

Fig. 4. Sample trace segments of measured liquid junction potential (LJP) shifts measured using a freshly-cut 3 M KCl-agar reference salt-bridge for two different NaF biionic solution combinations. The vertical grey bars represent the change-over period between control and test solutions when the tip of the 3 M KCl-agar salt-bridge is cut off by at least 5 mm. The traces differ slightly from those in Fig. 3, in that they have been digitally filtered (with a 50 Hz low-pass Gaussian filter) to reduce the increased noise obtained with the use of an Axopatch-1D amplifier for these measurements. The left panel shows a typical fairly rectangular response for the NaCl:NaF biionic measurement, whereas the right panel shows a typical more transient response for the NaI:NaF biionic measurement (see text for discussion).

Discussion). Nevertheless, it should be noted that the mobilities of Cs^+ and Cl^- are almost equal and that the combined contribution of both ions to LJPs is generally very small. As noted under *Experimental Protocol* for the CsCl:LiCl biionic, in which the mobilities of the two

Table 2. Corrected experimental measurements of liquid junction potentials (ΔV_{LJ}^{m}) in mV at 22 °C under dilution conditions for a range of alkali halides.

		$-\Delta V_{exp}$	Using activities			Using Concentrations			n
			ΔV_{3M}^{a}	ΔV_{LJ}^{ma}	ΔV_{LJ}^{pa}	ΔV_{3M}^{c}	ΔV_{LJ}^{mc}	ΔV_{LJ}^{pc}	
NaCl	0.50	−2.7	−0.6	−3.3	−3.2	−0.6	−3.3	−3.4	16
NaCl	0.25	−5.5	−1.1	−6.6	−6.5	−1.0	−6.5	−7.0	15
LiCl	0.50	−4.4	−0.7	−5.1	−5.1	−0.7	−5.1	−5.4	29
LiCl	0.25	−9.2	−1.3	−10.5	−10.4	−1.3	−10.5	−11.0	23
KCl	0.50	+0.1	−0.3	−0.2	−0.3	−0.3	−0.2	−0.3	9
KCl	0.25	+0.1	−0.6	−0.5	−0.6	−0.6	−0.5	−0.6	12
CsCl	0.50	+0.2	−0.2	+0.0	+0.1	−0.3	−0.1	+0.1	13
CsCl	0.25	+0.5	−0.5	+0.0	+0.1	−0.5	−0.0	+0.2	6
NaF	0.50	-0.6	-0.3	-0.9	-0.8	-0.3	-0.9	-0.8	13
NaF	0.25	-1.1	-0.6	-1.7	-1.6	-0.7	-1.8	-1.7	21

In all cases, the experimental SEMs for $-\Delta V_{exp}$ were ≤ 0.01 mV. All dilutions (Column 2) are given relative to 1.0 XCl or NaF as appropriate. The uncorrected experimental value, in mV, is $-\Delta V_{exp}$. ΔV_{3M} represents the calculated 3 M KCl reference correction. The corrected values are related to the raw experimental measurements by $\Delta V_{LJ}^{m} = -\Delta V_{exp} + \Delta V_{3M}$ (Eq. 1). The predicted ΔV_{LJ}^{p} is calculated using *JPCalcW*. Superscripts [a] and [c] indicate that the correction ΔV_{3M}, the corrected ΔV_{LJ}^{m} and the predicted ΔV_{LJ}^{p} were calculated using ion activities or concentrations, respectively. n represents the number of bracketed measurements of LJPs used for each pair of solutions. The relative mobility values for all the major ions were taken as those at 22 °C as given in Table 1, rather than the values at 25 °C. Expected errors due to measurement and calculation resolutions in ΔV_{exp} were ± 0.05 mV each for $-\Delta V_{exp}$, ΔV_{3M} and ΔV_{LJ}^{p}. Total errors expected for comparing ΔV_{LJ}^{m} and ΔV_{LJ}^{p} were ~ ± 0.1 mV. The relative mobility values for all the major ions were taken as those at 22 °C, as given in Table 1.

cations are very different, when the control/test duration ratio was increased (Fig. 3C), the small transient component to the ΔV_{exp} shifts, was much reduced, presumably because the CsCl salt-bridge composition has had time to equilibrate more fully to CsCl before being placed in contact again with LiCl and to more readily meet the requirement of junction solution layers being mixtures of the end solutions. In addition, the predicted LJP values of the NaI:NaF biionics were 0.3 mV more positive than the −5.1 mV measured value, again somewhat beyond the ± 0.1 mV resolution rounding error. This may reflect the purity of the two solutions (both only >99%) and state of hydration of the NaI·H_2O. Also, a slight transient LJP response was observed between the NaI and NaF solutions that was not observed between the NaCl and NaF solutions (Fig 4).

In contrast to the LJP measurements with solution dilutions, there was little difference between biionic LJP predictions and corrected measurements calculated using ion activities or ion concentrations, though the values

Table 3. Corrected experimental measurements of liquid junction potentials (ΔV_{LJ}^{m}) in mV at 22 °C for a range of alkali cation and halide anion pairs.

Solution Pairs		$-\Delta V_{exp}$	Using ion activities			Using ion concentrations			
			ΔV_{3M}^{a}	ΔV_{LJ}^{ma}	ΔV_{LJ}^{pa}	ΔV_{3M}^{c}	ΔV_{LJ}^{mc}	ΔV_{LJ}^{pc}	n
NaCl	KCl	−3.7	−0.8	−4.5	−4.5	−0.6	−4.3	−4.4	13
KCl	NaCl	+3.7	+0.8	+4.5	+4.5	+0.6	+4.3	+4.4	13
NaCl	LiCl	+2.1	+0.4	+2.5	+2.6	+0.3	+2.4	+2.5	7
KCl	LiCl	+5.9	+1.2	+7.1	+7.1	+0.9	+6.8	+6.9	7
CsCl	LiCl	+6.2	+1.3	+7.5	+7.7	+1.0	+7.2	+7.5	12
CsCl	NaCl	+4.0	+0.9	+4.9	+5.1	+0.7	+4.7	+5.0	10
CsCl	KCl	+0.2	+0.1	+0.3	+0.6	+0.1	+0.3	+0.6	11
NaCl	NaI	+0.2	+0.0	+0.2	+0.2	+0.0	+0.2	+0.1	8
NaCl	NaF	−3.7	−0.8	−4.5	−4.7	−0.6	−4.3	−4.6	11
NaI	NaF	−4.3	−0.8	−5.1	−4.8	−0.7	-5.0	−4.7	12

In all cases, the experimental SEMs for $-\Delta V_{exp}$ were ≤ 0.015 mV. As in Table 2, ΔV_{LJ}^{p} refers to predicted LJPs (calculated using *JPCalcW*), and the superscripts [a] and [c] indicate that the correction (ΔV_{3M}), corrected ΔV_{LJ}^{m} and predicted ΔV_{LJ}^{p} were calculated using ion activities or concentrations respectively. n represents the number of bracketed measurements of LJPs used for each pair of solutions. As in Table 2, the relative mobility values for all the major ions were taken as those at 22 °C rather than the values at 25 °C. Generally this only changed predicted values by ≤ 0.1 mV. The uncorrected experimental measurement, ΔV_{exp}, has an individual measurement (reading/calculation) precision of ± 0.05 mV and the calculated correction (using ion activities) for the LJP of the 3 M KCl salt-bridge, using the *JPCalcW* program, has a precision of ± 0.05 mV. Hence, the corrected experimental values using Eq. 1, $\Delta V_{LJ}^{m} = -\Delta V_{exp} + \Delta V_{3M}$, should allow for a combined precision error of ± 0.1 mV.

using activities displayed marginally better agreement (Table 3). However, this broad agreement is to be expected since the ionic strengths of each of these univalent salt solutions are virtually identical and ionic activities at the same ionic strength vary minimally between such salts.

Theoretical Calculations

The first section discusses the relationship between ion mobility values, needed for the LJP calculations, and measurements of limiting equivalent conductance. The second section then derives the equations for diffusion into and out of the 3 M KCl agar-salt-bridge, in order to give a rationale for lengths of salt-bridge that need to be cut off to provide a fresh 3 M KCl salt-bridge tip after different conditioning times in each solution.

Relative ion mobility values

Values of the mobility of ions relative to K^+ are needed both for the calculation of theoretical values of LJPs and also for the correction of experimental measurements of LJPs. The mobility of an ion can be calculated from the experimental measurement of its limiting equivalent conductance (Λ^0_X, for ion X), which can either be obtained from a number of published sources (e.g., Barry and Lynch 1991; Dean 1999; Keramidas et al. 1999; Ng and Barry 1995; Robinson and Stokes 1965; Vanysek 2002; see also: http://web.med.unsw.edu.au/phbsoft/mobility_listings.htm) or else by direct measurement (e.g., Ng and Barry 1995; Keramidas et al. 1999). The relationship between relative ion mobility, u_X, and Λ^0_X for ion X of valency z is derived in Appendix S1 of the ESM and shown to be given by:

$$u_X = [\Lambda^0_X / |z|] / \Lambda^0_K \qquad (4)$$

where Λ^0_K is the limiting equivalent conductivity of K^+ ions.

Electrolyte diffusion into and out of the 3 M KCl agar-salt-bridge

In order to calculate diffusion of test electrolytes into and KCl out of the 3 M KCl agar-salt-bridge, a correction is required for the effect of agar on the ion diffusion coefficients. Slade et al. (1966) have shown that the relative changes in ionic diffusion in agar solutions varies linearly with the % agar content of the solution and are independent of the nature of the ion, its concentration or the solution temperature. They have shown that the empirical relationship between the diffusion coefficient in the presence, $D(t,c,w)$, and in the absence, $D(t,c)$, of agar for any individual ion, is given by:

$$D(t,c,w) / D(t,c) = 1 - 0.023\, w \qquad (5),$$

where t and c represent the temperature and concentration of the electrolyte, and w is the %w/v (g/100ml) of agar in the solution. Hence, for a 4% content of agar in a solution the diffusion coefficient in the presence of agar is reduced to 0.908 of its free-solution value. At 20°C for 100 mM NaCl, $D_{NaCl} = 1.33\times10^{-5}$ cm^2s^{-1} in free solution (see Table 4), in the presence of 4% agar, $D_{NaCl(agar)} = 1.21\times10^{-5}$ cm^2s^{-1}. Similarly, $D_{LiCl(agar)} = 1.03\times10^{-5}$ cm^2s^{-1} and $D_{CsCl(agar)} = 1.54\times10^{-5}$ cm^2s^{-1} and between 2M to 3 M, $D_{KCl(agar)} \cong 1.64\times10^{-5}$ cm^2s^{-1}. As shown in Appendix 1, the situation for the test solute (electrolyte) diffusing from the solution bath into a cylindrical agar salt-bridge would be equivalent to that of solute diffusion into an infinite medium with a fixed concentration at x=0 and is given (Eq. 19) by:

$$C_s = C_{s0}\, erfc\left[\frac{x}{2\sqrt{D_s t}}\right], \qquad (6),$$

where C_s is the concentration of the test solute in the salt-bridge, x is the distance from the cut end of the salt-bridge in the test salt solution, t is the time from when the salt-bridge was placed in the solution, C_{s0} is the concentration of the test solution in the bath, D_s is the diffusion coefficient of the test solute in the agar salt-bridge and erfc is the complementary error function (see Abramowitz and Stegun (1965). It is reasonably assumed that at time $t = 0$, $C_s = 0$ for all $x > 0$ in the salt-bridge and that at $x = 0$, $C_s \cong C_{s0}$ for $t > 0$.

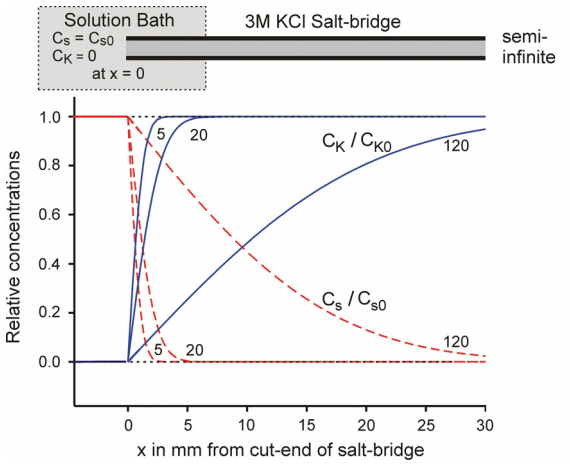

Fig. 5. A schematic diagram to indicate the relative concentration changes at the tip of an effectively semi-infinite 3 M KCl salt-bridge with the cut-end placed in a test salt solution bath (in this case of 150 mM NaCl) for 3 different conditioning times. The concentration of the test solute in the solution bath is considered to remain constant right up to the tip of the small salt-bridge, the salt-bridge to be initially composed of 3 M KCl, and the KCl concentration to remain at 0 within the solution bath. The relative concentration profiles (C_s/C_{s0} and C_K/C_{K0} for the NaCl and KCl salts, respectively, where C_{s0} represents the NaCl concentration within the solution bath, and C_{K0} the initial 3 M KCl concentration within the salt-bridge), were calculated assuming that the end of the salt-bridge had been in the test solution for three different conditioning times - 5 min, 20 min and 120 min, with these times being shown adjacent to the solute and KCl curves to which they refer (see also Table S3 in ESM). The diffusion coefficients of both NaCl and KCl were corrected for the reduction in diffusion coefficient produced by 4% (*w/vol*) agar. Diffusion coefficients were those at 20°C and corrected for 4% agar in the 3 M KCl salt-bridge ($D_{NaCl(agar)} = 1.21\times10^{-5}cm^2\ s^{-1}$ and $D_{KCl(agar)} = 1.64\times10^{-5}\ cm^2\ s^{-1}$; see Table 4). As indicated in the inset, initially ($t = 0$, $x=0$) within the 3 M KCl-agar salt-bridge, the concentration of KCl (C_{K0}) is 3 M and the concentration of test solute (C_s) is 0. At $x = 0$, for $t \geq 0$, $C_s = C_{s0}$ and the concentration of KCl (C_K) = 0.

As derived *de-novo* in Appendix 1 (Eq. 32), the situation for the 3 M KCl solution within the salt-bridge diffusing out of the tip of the KCl-agar salt-bridge is shown to be given by:

$$C_K = C_{K0}\, erf\left[\frac{x}{2\sqrt{D_K t}}\right], \qquad (7)$$

where now erf is the regular error function [related to erfc by erfc(z) = 1 − erf(z)], C_K is the concentration of the KCl in the salt-bridge for $x > 0$, C_{K0} is its initial concentration (3 M) for all $x > 0$ in the salt-bridge ($t = 0$), D_K is the diffusion constant of KCl in the agar salt-bridge and the other parameters are as before. It is assumed that the concentration of KCl at $x = 0$ is kept very close to 0, by rapid diffusion from the small aperture of the salt-bridge as a virtual point source into the large bath test solution, which will be considered to be NaCl for the purposes of this analysis. From Eqs. 6 and 7, and the above diffusion coefficients in agar at 20°C, we can calculate the changes in concentration profiles of test solute and "3 M" KCl in the salt-bridge with time (concentration profile differences between 20 and 22 °C will be very small). These concentration profiles are illustrated in Fig. 5 for a cut salt-bridge that has been in a solution of test solution of NaCl (150 mM) for 5, 20 and 120 minutes. For example, after 20 min, the concentration of NaCl 1 mm in from the end of the salt-bridge will have risen to 56% of the solute concentration in the bath solution (i.e., 84 mM for a 150 mM NaCl bath solution) and the KCl solution will have dropped to about 39% of its initial 3 M concentration at that same distance (to ~ 1.2 M). However, at 5 mm from the end of the salt-bridge, the NaCl concentration will be only 0.3% of the bath concentration and the KCl concentration will have only dropped to 98.9% of the original 3 M concentration (see Table S3 in the **ESM**). The concentration profiles at 20 min are also shown on an expanded time scale in Fig. S7 and given in Table S3 (in the **ESM**). After 120 min, there is extensive mixing of the bath and 3 M KCl solutions for a distance of up to about 25-30 mm (Fig. 5).

Table 4. Diffusion constants at 20°C converted from values at 25°C.

Salt	Conc (M)	λ^o_+ (20°C)	λ^o_- (20°C)	λ^o_+ (25°C)	λ^o_- (25°C)	D_{salt20}/D_{salt25}	D_{salt} (25)	D_{salt} (20)	D_{salt} (20) (4% agar)
LiCl	0.1	34.50	68.96	38.60	76.35	0.897	1.260	1.13	1.03
NaCl	0.1	44.89	68.96	50.10	76.35	0.899	1.483	1.33	1.21
KCl	2-3	66.64	68.96	73.50	76.35	0.905	2.0	1.8	1.64
CsCl	0.1	69.90	68.96	77.20	76.35	1.871	1.871	1.69	1.54

These values were obtained from Robinson and Stokes (1965; Table 11.2, P. 515) using the temperature dependency of limiting equivalent conductivities of the individual ions (from Robinson and Stokes, 1965; Appendix 6.2), since $D_{salt} = 2\times(\lambda^o_+\times\lambda^o_-)/(\lambda^o_+ + \lambda^o_-)$, where λ^o_+ and λ^o_- are the limiting equivalent conductivities of the appropriate cation and anion of the salt. D_{salt} units are 10^{-5} cm^{2}s^{-1}. The last column also gives the 20 °C value corrected for 4% (*w/vol*) agar (Eq. 5).

A summary of the validity of the use of the Henderson equation for calculating LJPs

The validity of the Henderson equation (Henderson, 1907, 1908, MacInnes, 1961) may seem questionable since it originated from a thermodynamic derivation of the pseudo steady-state potential across a junction between two solutions of different salt composition with different ionic mobilities, rather than being rigorously derived from electro-diffusion equations and electrostatic principles under dynamic conditions. We will briefly summarize here the discussion given in Appendix S2 of the accompanying Electronic Supplementary Material (ESM) which shows, maybe somewhat surprisingly given the evolving size of the unconstrained junction region, that there is very good justification for the validity for the Henderson equation under many pseudo steady-state conditions.

First of all empirically, as demonstrated in this paper, and in many others studies (e.g., Barry & Diamond, 1970; Ng & Barry, 1995; Keramidas et al., 1999; Sugiharto et al., 2010 and Barry et al., 2010) the Henderson equation has been very successful in predicting LJP experimental values. In addition, a vast amount of increasingly more rigorous derivations of electro-diffusion equations have now been applied to investigate the development of the LJP. In the 1960s and 1970s, Hafemann (1965), Hickman (1970) and Jackson (1974) variously used irreversible thermodynamics, numerical and analytical methods based on the Nernst-Planck equations and taking into account calculations of the electric field using Gauss' law or the related Poisson equation, together with perturbation analyses. They investigated the Type 1 dilution junction [A^+X^-(C1) || A^+X^- (C2)], for a uni-univalent electrolyte (A^+X^-) at two different concentrations (C1,C2), and the Type 2 biionic junction [A^+X^-|| B^+X^-], for two different uni-univalent electrolytes at the same concentration. In both cases, they showed for two such semi-infinite solutions in contact (an unconstrained junction), that the electric field profile in the contact region rapidly rises and reaches a sharp peak in a nanosecond timescale before starting to fall and flatten out as the junction region continues to expand. However, they also showed that the overall potential across the junction region, the LJP, rapidly rises asymptotically over tens of nanoseconds towards a steady maximum value, close to the value predicted by the Henderson equation. Recently, Compton and colleagues (Dickinson et al., 2010, Ward et al., 2010 and Zhurov et al., 2011) have used a more exact and rigorous Nernst-Planck-Poisson (NPP) finite difference numerical simulation system, together with perturbation analyses, to confirm and extend the basic conclusions of

the above earlier studies. They produced a complete quantitative simulation of the dynamic evolution of the LJP across an unconstrained junction (see also Perram and Styles, 2006; for their similar analysis of a constrained junction), together with the evolution of the profiles of the ionic concentrations and electric field across the expanding junction region, from the moment the two solutions first come into contact. Dickson et al. (2010), following Hickman (1970), also used perturbation analysis to show that for the Type 1 dilution junction, the LJP solution of the NPP equations for long times can be approximated by a power series, whose first time-independent term is the Henderson equation, with the other terms tending to rapidly go to zero as time increases, to give "exact" agreement with the Henderson equation at long enough times. In their simulation studies they showed that agreement between their experimentally simulated values and the Henderson equation was within 0.25%. For the Type 2 biionic junction, Dickson et al. (2010) showed that the LJP solution, required an additional perturbation involving diffusion coefficients, and demonstrated that agreement with the Henderson equation, while no longer exact, was still within 0.8% for all the cases they considered. For Type 3 bionic junctions [A^+X^-‖ B^+Y^-], with no common anion or cation, and a multilayer liquid junction, Ward et al. (2010) found that there could be even greater deviations from the Henderson equation. However, their calculations indicated that even for a hypothetical unbuffered [Na^+Acetate$^-$‖ K^+OH^-] junction, with very large differences in relative ionic mobilities (0.682, 0.556, 1.0, 2.69 respectively for the above ions; see ESM), the deviation from the Henderson equation was only 1.55% (20.4 mV compared to the value of 20.72 calculated from the Henderson equation). *It should be noted that the above mobility comments relate to the major ions in the solution. They do not apply to solutions with small concentrations of ions with very low or high mobilities, included with large concentrations of ions of more standard mobilities. The low concentrations of such ions would not be expected to significantly contribute to the LJP. In addition, for almost all relevant* ***major*** *ions in physiological solutions, the range of ion mobilities would be much less than in the above KOH case.* In summary, these informative theoretical studies on the evolution and underlying mechanisms of LJPs provide validity and a theoretical rationale for the use of the Henderson equation for calculating pseudo 'steady-state' LJPs in the double semi-infinite solution junction described above. Only small deviations are predicted in Type 2 (0.8%), and Type 3 (1.55%) junctions for large ion mobility differences with the caveat of larger deviations for greater mobility differences with the Type 3 junctions.

It should be noted that the interface between a small salt-bridge in contact with a large volume bath (as used in this present paper), should behave as a constrained boundary, tending to hold the composition at the interface close to the bath composition, whereas the salt-bridge would behave as a semi-infinite solution. This should result in a much simpler single semi-infinite system rather than two semi-infinite solutions in contact, with the pseudo steady-state LJP of such a junction even more closely approximated by the Henderson equation, maybe at least halving the deviations described above. Such a system could be a worthy subject for an NPP analysis.

Other issues, which might possibly affect the accuracy of the calculated LJPs in the salt-bridge–solution bath system, not taken into account in the above theoretical studies, are non-electrical cross-coupling interactions between ion fluxes, effects of solvent convection on ion fluxes (e.g., Mori et al., 2011) and the presence of high concentrations of sucrose in dilution solutions. These are discussed in Appendix S2 in the ESM in the light of some additional LJP dilution measurements in pure NaCl solutions (Table S4) and are summarized here. The equality of the absolute values of the measured LJPs for 150:300 and 150:75 NaCl dilutions suggest no significant ion flux cross-coupling, which would otherwise be expected to increase at higher average solution concentrations. Given the open nature of the gelled agar salt-bridges, the reflection coefficient for sucrose would be expected to be zero and hence not to generate any osmotic volume flow across the junction region. This was experimentally validated by the agreement between measured and calculated dilution NaCl LJPs in the presence (Table 2) and absence (Table S4) of sucrose. This result was also consistent with sucrose not having any noticeable affect on ion activities, though LJPs are not very sensitive to small changes in ion activity coefficients.

Solvent convection effects could possibly be present with a pipette reference electrode in contact with a solution bath, if the solution in the pipette were free-flowing under a hydrostatic gradient, to minimize history-dependent effects. In such a situation, the resultant volume flow could, at least in principle, have some convective effect on the magnitude of the LJP. This is avoided by using an agar salt-bridge.

Discussion

We describe here a detailed method and theory for reliably and accurately measuring liquid junction potentials (LJPs) that arise when two different solutions come in contact. Knowing the value of such potentials is critical in patch-clamp measurements and cellular electrophysiology, for example where one wishes to know the precise value of the membrane potential or the change in membrane potential following a change in the composition of the bath solution. Our method uses two agar salt-bridges: one similar in composition to the control solution, and the other a 3 M KCl-agar reference salt-bridge. Critical to the successful use of the 3 M KCl reference bridge are two points. Firstly, the 3 M KCl salt-bridge tip needs to be freshly cut prior to each solution transfer. Secondly, the shift in potential at the 3 M KCl reference salt-bridge (ΔV_{3M}) needs to be taken into account for such measurements. This ΔV_{3M} potential is small and well-defined because of both the high relative concentration of K^+ and Cl^- dominating the diffusion potential, and because these two ions have similar, but not equal, mobilities ($u_{Cl}/u_K \approx 1.04$). It can be readily calculated, as we show here. The procedures outlined in this paper are validated by showing excellent agreement between the experimental values, and those predicted

theoretically using ion activities (particularly for dilution potentials) rather than ion concentrations. This has been shown using anions and cations with a range of mobilities.

In addition, we have described how the use of the Henderson equation for calculating pseudo 'steady-state' LJPs has been validated over the last few decades by the rigorous Nernst-Planck-Poisson and other numerical simulation and analytical studies of the evolution of LJPs. These studies, all with two semi-infinite solutions in contact, have predicted "exact" agreement with the Henderson equation for Type 1 LJPs (dilutions), and very good approximations for Types 2 and 3 LJPs (biionics), with the latter two agreeing within 0.8% and 1.55% (e.g., 0.3 mV in 20.4 mV), respectively, for even the extreme cases considered. However, we expect that LJPs for an agar salt-bridge in a solution bath should behave like a single semi-infinite solution with a constrained solution boundary, and the above predicted errors be at least halved. The previous section and Appendix S2 of the ESM, with additional pure NaCl solution LJP data, also showed that osmotic and convective flow effects are not a problem for salt-bridges, though convective flow may affect LJPs when using free-flowing pipettes.

From our point of view, the main reason for wanting to directly measure LJPs was to validate calculated LJP values. Alternatively, if the mobilities of one or more of the major ions are not known accurately, an uncorrected value of the LJP can be directly measured. In the absence of any ΔV_{3M} correction, this will provide at least some estimate of the LJP (e.g., cp. $-\Delta V_{exp}$ and ΔV_{LJ}^{ma} values in Tables 2 and 3). However, to get an accurate measurement of the LJP, there still needs to be a correction for the ΔV_{3M} contribution to the LJP. Fortunately, as may be seen from Tables 2 and 3, the contribution of the ΔV_{3M} term is a second order effect (see Tables 2 and 3) and only a rough estimate of the non-KCl ion mobilities is needed (e.g., from known mobilities of ions of a similar size and properties) to get a reasonable estimate of the ΔV_{3M} contribution to the LJP. For example from Table 2, for 0.25 dilution LJPs, ΔV_{3M} corrections differed little between LiCl (-1.3 mV; $u_{Li}/u_K \approx 0.52$) and NaCl (-1.0 mV; $u_{Na}/u_K \approx 0.68$). Similarly for biionic LJPs from Table 3, ΔV_{3M} corrections differed little between CsCl:LiCl (+1.0 mV) and CsCl:NaCl (+0.7 mV). Further discussion of how to get a more accurate estimate of ΔV_{3M} and the use of LJP measurements to estimate ion mobility values is given in Appendix S3 in the ESM.

The Henderson equation can, in principle, handle any mixture of monovalent and divalent ions. Experimental verification of the equation was checked for values of LJPs of 0.5 and 0.25 NaCl dilution potentials (from 145 mM NaCl +HEPES etc, as in Table 2) in the absence (-6.4 mV) and presence (-5.8 mV) of 4 mM $CaCl_2$ using an earlier slightly less optimised version of the cut 3 M KCl salt-bridge technique. The results indicated agreement (within 0.1 mV) between the corrected experimental and predicted values of the LJPs [e.g., -6.4 mV and -6.4 mV (+ 0 $CaCl_2$) and -5.8 mV and -5.7 mV (+ 4 mM $CaCl_2$) for the 0.25 dilutions, in each case for the ΔV_{LJ}^{ma} and ΔV_{LJ}^{pa} respectively; Table 2 of Sugiharto et al., 2010].

The aim of our study was to accurately measure the shift in the LJP of a salt-bridge when it is transferred from one solution (control, e.g., 1.0 NaCl) to a new solution (test, e.g., 1.0 LiCl). To record this shift in LJP requires a reference electrode. In principle, a 3 M KCl reference salt-bridge-Ag/AgCl electrode would seem to be ideal because of its high concentration and near-similarity of the K^+ and Cl^- mobilities, but such a reference salt-bridge suffers from history-dependent effects, as demonstrated in Fig. 3. However, we have demonstrated that these history-dependent effects can be eliminated by freshly cutting the 3 M KCl tip. This solution history-dependence has previously been demonstrated in a slightly different way for pairs of saturated KCl reference salt-bridges in some alkali cation chloride solutions, by comparing the potential difference between them before and after the ends were cut off (Figs. 3 and 4 of Barry and Diamond 1970) and measuring the LJPs with Ag/AgCl electrodes, with substantial corrections for their electrode potentials.

The theoretical analysis of test-solute diffusion into, and KCl diffusion out of, a 3 M KCl salt-bridge given in Appendix 1 showed clearly that a 5 mm length cut off the end of the salt-bridge should be adequate for ensuring a fresh 3 M KCl tip when the 3 M KCl salt-bridge had been left in its previous test solution for up to about 20 min. We generally used 6-8 mm cuts with 3 M KCl salt-bridges left in test solutions for less than 10 min. We also found that after the 3 M KCl salt-bridge had been left in its previous test solution for a more extended period of an hour or two while the test salt-bridge was equilibrating, that it needed to be cut by more than 20 mm, before we got maximal and stable potential rectangular shifts in response to solution changes (Fig. S2 in the **ESM**).

An alternative approach to a freshly cut 3 M KCl-agar salt-bridge would be to use a 3 M KCl microelectrode. The microelectrode tip and shank diameter would need to be large enough to minimize surface tension in the pipette shank and ensure a free-flowing KCl through the tip. However a large diameter shank and tip has the potential problem of KCl leaking into the solution and contaminating its composition. Neher (1992) suggests a patch-clamp pipette with a 2 μm bore as a suitable trade-off, and such pipettes have been successfully used for LJP measurements. However, the system will also result in an offset Ag/AgCl electrode potential of about 70 mV between a typical 150 mM XCl salt-bridge electrode and a reference 3 M KCl patch-pipette, and this needs to remain stable to within about 0.1 mV during the measurements for very accurate measurements. Also, if the pipette solution were not free flowing, or became non-free flowing, during the measurements, then the measurements could become invalid. The freshly-cut 3 M KCl-agar salt-bridge approach outlined here provides a simpler and very reliable alternative that virtually eliminates the electrode offset potential, reduces the chance of solution contamination by KCl, and has no need for a free-flowing pipette-type condition.

Using this optimised simple technique, we have measured LJPs for a number of salt solution dilutions and biionic solution combinations and compared the corrected experimental measurements of the LJPs with those values

calculated with the *JPCalcW* program that uses the Henderson equation for such calculations (Eqs. 2 and 3 and Barry and Lynch 1991). NaCl, KCl, LiCl and CsCl salts were chosen because of their common use in ion permeation and selectivity studies, and because their ion mobilities and activity coefficients are all accurately known and span a range of values. Two other halide ions, F^- and I^- were chosen that had the smallest and largest mobilities of the group (Table 1). For the dilution potential experiments, the measured values (corrected for 3 M KCl LJPs) give excellent agreement with the predicted LJP values, calculated using ion activities, (Table 2; cf. ΔV_{LJ}^{ma} and ΔV_{LJ}^{pa}) within expected rounding errors (± 0.1 mV) for all the measurements done for this article. There was also excellent agreement between calculated and measured (and corrected) LJPs for the biionic solutions for LiCl, NaCl and KCl, and for NaCl:NaI and NaCl:NaF, with the measured values agreeing within the expected error of ± 0.1 mV (Table 3). However, for the three biionic combinations which involved CsCl, the predicted LJP was consistently just greater in magnitude than the corrected measured value, and expected ± 0.1 mV error, by 0.1 mV (CsCl:LiCl and CsCl:NaCl) and 0.2 mV (CsCl:KCl) (Table 3). These differences are still small, but the fact that they just seem to occur with CsCl biionics, suggests that they may be related to the mobility properties of Cs^+. Indeed, the differences could be accounted for if the mobility of Cs^+, with its extremely loosely bound hydration shell, under typical biionic and dilution concentration gradients, were slightly less (u_{Cs}/u_K = 1.040) than the value determined from its limiting equivalent conductance (u_{Cs}/u_K = 1.049) in the presence of a relatively large applied electric field (see section on *Possible effect of electric field on Cs^+ mobility* in the **ESM**). In addition, the predicted LJP values of the NaI:NaF biionics were 0.3 mV more positive than the −5.1 mV measured value. This may similarly reflect a more loosely bound hydration shell for this large anion.

However, for **biionic** LJPs**,** the use of **ion concentrations** was almost as good as the use of **ion activities** for predicting their LJPs, the values generally agreeing to within 0.2 mV or less. This is also to be expected since the ionic strengths of biionic solutions are essentially the same, and hence the activity coefficients should be very similar and almost cancel out.

In addition, unless the highest precision is needed for comparing experimental and theoretical values of relative ion mobilities, the values at 25 °C should be quite adequate in the range of 20 °C to 30 °C.

In conclusion, the results presented here for agar salt-bridge LJPs, together with the published results of rigorous theoretical analyses and numerical Nernst-Planck-Poisson simulations of LJPs, validate, to an impressive degree, the reliability of predicted liquid junction potentials calculated using the Henderson equation, when ion mobilities are accurately known. We demonstrate two important points for direct LJP measurements: 3 M KCl-agar reference salt-bridges with freshly-cut tips should be used, and the small, but significant, LJP correction for the 3 M KCl-agar reference salt-bridge needs to be taken into account.

Appendix 1: A mathematical description of the diffusion of a test electrolyte solution into a 3 M KCl-agar salt-bridge, and of KCl out of that salt-bridge into the electrolyte solution.

by Peter H. Barry

The inset at the top of Figure 5 shows a schematic diagram of the typical experimental situation that needs to be investigated. The aim is to derive the diffusion of the test solute into the agar salt-bridge as a function of distance, x, and to derive the concurrent diffusion of KCl out of the 'point source' salt-bridge into the 'infinite-volume' bath solution. The freshly-cut 3 M KCl agar salt-bridge is placed into the solution bath for a conditioning time t. It is expected that under such conditions, at x = 0, the test solute concentration C_s will remain constant with time and approximately equal to the bath concentration, C_{s0}. Similarly, the bath KCl concentration, C_{KCl} at x = 0, will, to a very good approximation, remain = 0. Initially, the concentration of KCl will be uniformly 3 M within the agar salt-bridge (x>0, t = 0). From that time on (t > 0), the diffusion situation within that salt-bridge, should be equivalent to that of a semi-infinite medium, with diffusion only in the x direction, the test solute diffusing into the salt-bridge and KCl diffusing out of it. The diffusion of each solute will be independent and both diffusion problems are considered separately below.

Diffusion of the test solute into the 3 M KCl salt-bridge

The partial differential equation that describes diffusion of the test solute along the salt-bridge as a function of time and distance is:

$$\frac{\partial C_s}{\partial t} = D_s \frac{\partial^2 C_s}{\partial x^2} \tag{8}$$

where C_s and D_s represent the concentration and diffusion coefficient of the test solute, t represents the time, as indicated above, and x the distance as shown in Fig 5.

As indicated above, the boundary and initial conditions are given by Eqs. 9 and 10 respectively:

$C_s = C_{s0}$ at $x = 0$, for all $t \geq 0$ (9)

$C_s = 0$ at $x > 0$, for $t = 0$ (10)

A useful and effective way of solving such diffusion equations is to use the Laplace transform approach, which initially converts the partial differential equation in time and space to an ordinary differential equation in space (here just x), and then do the inverse transform to obtain the full solution in time and space. This Laplace transform requires multiplying each term in Eq. 8 by e^{-pt}, where p is a suitably large positive number, and integrating the resultant term between 0 and ∞ with respect to t. Initially rearranging, this becomes:

$$D_s \int_0^\infty e^{-pt} \frac{\partial^2 C_s}{\partial x^2} dt - \int_0^\infty e^{-pt} \frac{\partial C_s}{\partial t} dt = 0 \quad (11)$$

The first term becomes

$$D_s \int_0^\infty e^{-pt} \frac{\partial^2 C_s}{\partial x^2} dt = D_s \frac{\partial^2}{\partial x^2} \int_0^\infty C_s e^{-pt} dt = D_s \frac{d^2 \overline{C}_s}{dx^2} \quad (12)$$

where the bar above the C_s indicates the transformed C_s, now only dependent on distance, x For the second term in Eq. 11, we have, on integrating by parts:

$$\int_0^\infty e^{-pt} \frac{\partial C_s}{\partial t} dt = [C_s e^{-pt}]_0^\infty + p \int_0^\infty C_s e^{-pt} dt = p\overline{C}_s \quad (13)$$

The term in brackets disappears since $C_s = 0$, when $t = 0$ from initial conditions (Eq. 10). Hence we have from Eqs. 11-13 that:

$$D_s \frac{d^2 \overline{C}_s}{dx^2} = p\overline{C}_s \quad (14)$$

From the boundary condition at $x = 0$ (Eq. 9), we have that $C_s = C_{s0}$ and taking the Laplace transform of this equation, we have that

$$\overline{C}_s = \int_0^\infty C_{s0} e^{-pt} dt = \frac{C_{s0}}{p} \quad (15)$$

If we define $q^2 = p/D_s$ then we can write Eq. 14 as

$$\frac{d^2 \overline{C}_s}{dx^2} = q^2 \overline{C}_s \quad (16)$$

Eq. 16 has a simple exponential solution, $\overline{C_s} = Ae^{-ax}$, where A and a are constants to be evaluated after substituting into Eq. 16, which results in:

$$\frac{d^2 \overline{C}_s}{dx^2} = Aa^2 e^{-ax} = a^2 \overline{C}_s \quad (17)$$

By comparing Eqs. 16 and 17, $a = q$, so that the solution is $\overline{C}_s = Ae^{-qx}$. The constant A can then be determined from the initial boundary condition in Laplacian space (Eq. 15), since when $x = 0$, $\overline{C}_s = A$. Thus $A = C_{s0}/p$ and the solution (in Laplacian space) for all x becomes:

$$\overline{C}_s = \frac{C_{s0}}{p} e^{-qx} \quad (18)$$

where $q^2 = p/D_s$. As Crank (1975) indicates the inverse Laplace transform for Eq. 18 is of the form

$$C_s = C_{s0}\, erfc\left[\frac{x}{2\sqrt{D_s t}}\right] \quad (19)$$

where erfc is the complementary error function (see Abramowitz and Stegun (1965).

Diffusion of KCl from the 3 M KCl salt-bridge

The partial differential equation that describes KCl diffusion along the salt-bridge (and into the solution bath) as a function of distance and time is:

$$\frac{\partial C_{\mathrm{K}}}{\partial t} = D_{\mathrm{K}} \frac{\partial^2 C_{\mathrm{K}}}{\partial x^2} \tag{20}$$

where C_{K} and D_{K} represent the concentration and diffusion coefficient of KCl, with the other variables as defined for the diffusion of test solute above, and as shown in the inset at the top of Fig. 5.

As indicated earlier in this appendix for KCl diffusion from the salt-bridge, the boundary and initial conditions are given by Eqs. 21 and 22 respectively:

$C_{\mathrm{K}} = 0$ at $x = 0$, for all $t \geq 0$ (21)

$C_{\mathrm{K}} = C_{\mathrm{K0}}$ at $x > 0$, for $t = 0$ (22)

The initial condition is unusual, since most diffusion problems start with a 0 solute concentration for $t = 0$. However, the problem can still be solved using Laplace transforms. Taking the Laplace transform of Eq. 20,

$$D_{\mathrm{K}} \int_0^\infty \mathrm{e}^{-pt} \frac{\partial^2 C_{\mathrm{K}}}{\partial x^2} \mathrm{d}t - \int_0^\infty \mathrm{e}^{-pt} \frac{\partial C_{\mathrm{K}}}{\partial t} \mathrm{d}t = 0 \tag{23}$$

The first term in Laplacian space now becomes

$$D_{\mathrm{K}} \int_0^\infty \mathrm{e}^{-pt} \frac{\partial^2 C_{\mathrm{K}}}{\partial x^2} \mathrm{d}t = D_{\mathrm{K}} \frac{d^2 \overline{C}_{\mathrm{K}}}{dx^2} \tag{24}$$

For the second term in Eq. 23, we have, on integrating by parts:

$$\int_0^\infty \mathrm{e}^{-pt} \frac{\partial C_{\mathrm{K}}}{\partial t} \mathrm{d}t = [C_{\mathrm{K}} \mathrm{e}^{-pt}]_0^\infty + p \int_0^\infty C_{\mathrm{K}} \mathrm{e}^{-pt} \mathrm{d}t = -C_{K0} + p\overline{C}_{\mathrm{K}} \tag{25}$$

However, the term in brackets no longer disappears, since when $t = 0$ from initial conditions (Eq. 22), $C_{\mathrm{K}} = C_{\mathrm{K0}}$. Hence we have from Eqs. 24-25 that:

$$D_{\mathrm{K}} \frac{d^2 \overline{C}_{\mathrm{K}}}{dx^2} - p\overline{C}_{\mathrm{K}} = -C_{K0} \tag{26}$$

From the boundary condition at $x = 0$ (Eq. 30), we have that $C_{\mathrm{K}} = 0$ and taking the Laplace transform of this equation, we have that

$$\overline{C}_{\mathrm{K}} = 0 \text{ at } x=0 \tag{27}$$

Defining $q^2 = \mathrm{p}/D_{\mathrm{K}}$ then we can write the homogeneous part of Eq. 26 as

$$\frac{d^2 \overline{C}_{\mathrm{K}}}{dx^2} - q^2 \overline{C}_{\mathrm{K}} = 0 \tag{28}$$

As before, Eq. 28 has a simple exponential solution of the form, $\overline{C}_{\mathrm{K}} = A\mathrm{e}^{-ax}$, where A and a are constants that need to be evaluated. As before, by substituting for this solution into Eq. 28, $a = q$, so that the solution is $\overline{C}_{\mathrm{K}} = A\mathrm{e}^{-qx}$. To determine A we need to add the specific solution of equation Eq. 26, which is that

$$\overline{C}_{\mathrm{K}} = \frac{C_{K0}}{p} \tag{29}$$

to the solution of the homogeneous equation to give the full solution as:

$$\overline{C}_{\mathrm{K}} = A\mathrm{e}^{-qx} + \frac{C_{K0}}{p} \tag{30}$$

Using the boundary condition that $\overline{C}_K = 0$ at x = 0, from Eq. 29, $A + \frac{C_{K0}}{p} = 0$, so $A = -\frac{C_{K0}}{p}$, hence the solution in Laplacian space is

$$\overline{C}_K = C_{K0}[\frac{1}{p} - \frac{e^{-qx}}{p}] \quad (31)$$

The inverse transform of 1/p is 1 and that of e^{-qx}/p is of the same form as in Eq. 18, the full solution now becomes for the KCl diffusion out of the salt-bridge

$$C_K = C_{K0}[1 - erfc\left[\frac{x}{2\sqrt{D_K t}}\right]] = C_{K0}\, erf\left[\frac{x}{2\sqrt{D_K t}}\right], \quad (32)$$

where erf is the regular error function [related to erfc by erfc(z) = 1 − erf(z)], C_K is the KCl concentration in the salt-bridge for $x > 0$, C_{K0} is its initial KCl concentration (3 M) for all $x > 0$ in the salt-bridge ($t = 0$), D_K is the KCl diffusion constant in the agar salt-bridge and the other parameters are as before. It is assumed that the KCl concentration at $x = 0$ is kept very close to 0, by rapid diffusion from the small aperture of the salt-bridge as a virtual point source into the large bath solution.

From Eqs. 19 and 32, and the above diffusion coefficients, we can calculate the changes in concentration profiles of test solute and "3 M" KCl in the salt-bridge with time. The implications of these equations are discussed in the **Theoretical Calculations** section.

Electronic supplementary material is appended at the end of this article.

References

Abramowitz M, Stegun IA (1965) Handbook of mathematical functions. Dover Publications, New York (with corrections, 1969).

Barry PH (1994) JPCalc - a software package for calculating liquid junction potential corrections in patch-clamp, intracellular, epithelial and bilayer measurements and for correcting junction potential measurements. J Neurosci Methods 51:107-116

Barry PH, Diamond JM (1970) Junction potentials, electrode potentials, and other problems in interpreting electrical properties of membranes. J Membrane Biol 3:93-122

Barry PH, Lynch JW (1991) Topical Review. Liquid junction potentials and small cell effects in patch clamp analysis. J Membrane Biol 121:101-117

Barry PH, Sugiharto S, Lewis TM, Moorhouse AJ (2010) Further analysis of counterion permeation through anion-selective glycine receptor channels. Channels 4:142-149

Crank J (1975) The mathematics of diffusion. 2nd Ed., Oxford University Press, London

Dean JA (1999) Lange's handbook of chemistry, 15th Edition, McGraw-Hill, New York

Dickinson EJF, Freitag L, Compton RG (2010) Dynamic theory of liquid junction potentials. J Phys Chem 114:187-197

Hafemann DR (1965) Charge separation in liquid junctions. J Phys Chem 69:4226-4231

Henderson P (1907) Zur thermodynamic der Flüssigkeitsketten. Z Phys Chem 59:118-127

Henderson P (1908) Zur thermodynamic der Flüssigkeitsketten. Z Phys Chem 63:325-345

Hickman HJ (1970) The liquid junction potential - the free solution junction. Chem Eng Sci 25:381-398

Jackson JL (1974) Charge neutrality in electrolyte solutions and the liquid junction potential. J Phys Chem 78:2060-2064

Keramidas A, Kuhlmann L, Moorhouse AJ, Barry PH (1999) Measurement of the limiting equivalent conductivities and mobilities of the most prevalent ionic species of EGTA ($EGTA^{2-}$ and $EGTA^{3-}$) for use in electrophysiological experiments. J Neurosci Method 89:41-47

MacInnes DA (1961) The principles of electrochemistry. Dover Publications, Inc. New York

Mori Y, Liu C, Eisenberg RS (2011) A model of electrodiffusion and osmotic water flow and its energetic structure. Physica D 240: 1835-1852

Neher E (1992) Correction for liquid junction potentials in patch clamp experiments. Meth Enzym 207:123-131

Neher E (1995) Voltage offsets in patch-clamp experiments. In: Single-channel recording, 2nd Ed, eds. B. Sakmann and E. Neher, Plenum Press, New York

Ng B, Barry PH (1995) The measurement of ionic conductivities and mobilities of certain less common organic anions needed for junction potential corrections in electrophysiology. J Neurosci. Method 56:37-41

Perram JW, Stiles PJ (2006) On the nature of liquid junction and membrane potentials. Phys Chem Chem Phys 8:4200-4213

Robinson RA, Stokes RH (1965) Electrolyte solutions, 2nd Ed. Revised. Butterworths. London

Slade AL, Cremers AE, Thomas HC (1966) The obstruction effect in the self-diffusion coefficients of sodium and cesium in agar gels. J Phys Chem 70:2840-2844

Sugiharto S, Carland JE, Lewis TM, Moorhouse AJ, Barry PH (2010) External divalent cations increase anion-cation permeability ratio in glycine receptor channels. Pflügers Arch 460:131-152

Vanysek P (2002) Ionic conductivity and diffusion at infinite dilution. In: CRC Handbook of chemistry and physics (83rd Edn; ed. D.R. Lide), CRC Press, Boca Raton

Ward KR, Dickinson EJF, Compton RG (2010) Dynamic theory of type 3 liquid junction potentials: formation of multilayer liquid junctions. J. Phys Chem B 114: 4521–4528

Zhurov K, Dickinson EJF, Compton RG (2011) Dynamics of ion transfer potentials at liquid-liquid interfaces: the case of multiple species. 115: 12429–12440

Electronic supplementary material (ESM) to follow

Electronic Supplementary Material (ESM)
Solutions, Ag/AgCl electrodes, Ion activity calculations, Extra Figures and Data tables

An optimised 3M KCl salt-bridge technique to measure and validate theoretical liquid junction potential values in patch-clamping by Peter H Barry, Trevor M. Lewis and Andrew J. Moorhouse

This electronic supplementary material is to accompany the above article (Barry et al., 2013; DOI 10.1007/s00249-013-0911-3).

Salts and solutions

The NaCl (99.9% purity) and KCl (99.8% purity), Analytical Grade, came from Ajax Finechem (www.ajaxfinechem.com). The CsCl (99.9% purity) came from Sigma-Aldrich and was stored in an electrical dessicator (Secador, John Morris Scientific P/L) prior to use. Because of the hygroscopic nature of LiCl and the humidity of the laboratory, LiCl solutions were made up from commercial 8M LiCl solutions (Sigma_Aldrich; Molecular Biology Grade, ≥ 99%; checked by Sigma using $AgNO_3$ titration) which were first diluted to 400 mM stock solution and then further diluted volumetrically to their final concentrations. The NaI and NaF salts also came from Sigma-Aldrich and were ≥ 99% pure.

Production of Ag/AgCl electrodes

For the XCl electrode-salt bridge combination, where X refers to the alkali cations, Li^+, Na^+, K^+ or Cs^+, the Ag/AgCl electrode was made from sterling Ag wire electroplated in 0.1 M HCl. The Ag wire was physically cleaned with fine wet-and-dry sandpaper (400 grit) and handled with rubber gloves to avoid getting any grease from fingers on it. It was then washed in reverse osmosis (RO) water and dried with laboratory wipes. A few Ag wires (1-3 at a time) were then chlorided in 0.1 M HCl by passing unidirectional current between them (as the anode) and a second Ag electrode as the cathode, at fairly low current density 1-10 $mA.cm^{-2}$ for a number of minutes until the electrodes became a uniform mauve-brown. The Ag/AgCl wires are then washed in RO water. Note that reversing the current during electroplating is not recommended for making good potential measuring electrodes (e.g., Ives and Janz, 1961).

One of the Ag/AgCl wires is then placed in a modified glass Pasteur pipette, with a major part of the fine end of the pipette removed and the tip heat-polished, and the non-chlorided end of the Ag wire taped with a strip of plastic insulating tape to the outside of the pipette to hold it in place, as shown in Fig. S1. The pipette is then filled by syringe, from the larger diameter end, with a simple molten 150 mM XCl solution to which about 4% agar has been added (%wt/vol, i.e., ~4 g/100 ml; with the agar previously dissolved in the XCl by bringing it slowly to the boil) and allowed to cool and gell. The pipette is then sealed at the air-Ag/AgCl-agar-salt interface by a silicon rubber compound (Sylgard, Dow Corning) to minimize electrode deterioration and the electrode stored in a container with 150 mM XCl.

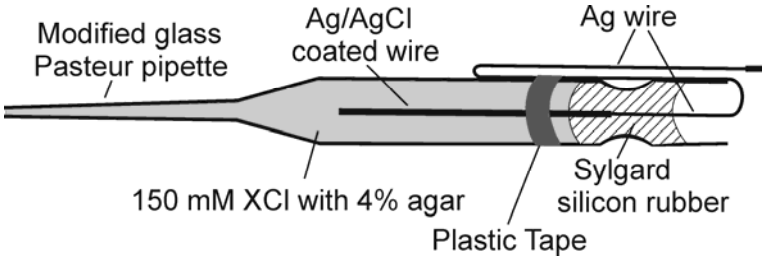

Fig. S1. *A schematic diagram of a 150 mM XCl Ag/AgCl electrode made from a modified glass Pasteur pipette and used for the measurements in the accompanying paper.*

The potential V_e of the Ag/AgCl single junction electrode is given by:

$$V_e = V_o^{Ag} - (RT/F) \ln (a_{Cl}) \quad \text{(S1)}$$

Where V_e represents the potential of the electrode with respect to the solution, V_o^{Ag} represents the standard electrode potential of the electrode and a_{Cl} the activity of Cl^- in the gelled solution in the electrode, and R, T and F have their usual significance of gas constant, Temp in K and Faraday.

Ion activity calculations

In order to determine the activity of ions in the solutions, it is necessary to determine first the ionic strength of the solutions, *I*, taking into account the contribution of all monovalent and divalent ions. *I* will be determined from the equation:

$$I = \sum_i \frac{C_i z_i^2}{2} \quad \text{(S2)}$$

where C_i is the concentration of each ion i in the solution and z_i is their valency. Given the relatively small proportion of ions like $HEPES^-$ and Ca^{2+} ions in the predominantly XCl solutions, where X represents the predominant cation in the solution (e.g., Na^+, K^+, Li^+ or Cs^+), the activity coefficient was taken from published data. In order to calculate individual ion activities, it can also be reasonably assumed that the interionic forces affect anion and cation equally and hence that the Guggenheim assumption should apply (MacInnes, 1961), which indicates that for a uni-univalent electrolyte, the individual ion activity coefficients (γ) will be the same, so that, for example, in an NaCl solution $\gamma_{Na} = \gamma_{Cl}$. In each case, the ion activity, a, will be related to the ion concentration, C, by:

$$a = \gamma C \quad \text{(S3)}$$

Estimates of ionic strength for some NaCl solutions are later shown in Table 1.

LiCl solutions. Likewise, the published activity data (between 10 and 200 mM) of Robinson & Stokes 1965; Table 9 of Appendix 8.7) at the temperature of the solution freezing point (within 0.2 % of the value at 25 ^oC for 100 mM; Table 9 of Appendix 8.10) was used by Barry et al. (2010) to show that the activity coefficients (γ) in LiCl solutions are fitted by the following relationship:

$$\gamma = 0.9895 - 0.9659x + 1.0232x^2 \quad \text{(S4)}$$

where $x = \sqrt{m}$ LiCl, and m is the molal concentration of LiCl, and is approximated by I, so that $x \cong \sqrt{I}$. For simplicity, m was approximated by molar (M) concentrations, the errors generally being less than 0.2% and the relative errors in final activities being much less than this.

NaCl solutions. The published activity data (between 20 and 200 mM) of Robinson & Stokes (1965; Table 1 of Appendix 8.9 and Table 10 of Appendix 8.1) at 25 ^oC was fitted using SigmaPlot by Sugiharto et al.(2010) to show that the activity coefficients (γ) in NaCl solutions are fitted by the following relationship:

$$\gamma = 0.9907 - 0.940x + 0.830x^2 \quad \text{(S5)}$$

where $x = \sqrt{m}$ NaCl, and is similarly approximated by $\sqrt{I}$, as in the case of LiCl above.

KCl solutions. Similarly, the published activity data (between 20 and 190 mM) of Robinson & Stokes (1965; Table 1, Appendix 8.9 and Table 11, Appendix 8.10) at 25 ^oC was used by Barry et al. (2010) to show that the activity coefficients (γ) in KCl solutions are fitted by the following relationship:

$$\gamma = 0.9908 - 0.9464x + 0.7586x^2 \quad \text{(S6)}$$

where $x = \sqrt{m}$ KCl, is similarly approximated as $\sqrt{I}$.

CsCl solutions. Similarly, the published activity data (between 17 and 193 mM) of Cui et al. (2007) at 25 ^{o}C was used by Barry et al. (2010) to show that the activity coefficients (γ) in CsCl solutions are fitted by the following relationship:

$$\gamma = 0.9814 - 0.9107x + 0.6105x^2 \quad \text{(S7)}$$

where $x = \sqrt{m}$ CsCl, is similarly approximated as $\sqrt{I}$. Note that the equivalent equation given in the above paper was for an extended concentration range, although the values used in their tables were the more accurate figures fitted over the limited range using the parameters of Eq. S7, as used in this present paper.

NaI solutions. The published activity data (between 100 and 400 mM) of Robinson & Stokes (1965; Table 11, Appendix 8.10) at 25 ^{o}C were used to show that the activity coefficients (γ) in NaI solutions are fitted by the following relationship:

$$\gamma = 0.9353 - 0.6095x + 0.4435x^2 \quad \text{(S8)}$$

where $x = \sqrt{m}$ NaI, is similarly approximated as $\sqrt{I}$.

NaF solutions. The published activity data (between 100 and 400 mM) of Robinson & Stokes (1965; Table 11, Appendix 8.10) at 25 ^{o}C were used to show that the activity coefficients (γ) in NaI solutions are fitted by the following relationship:

$$\gamma = 0.9403 - 0.6519x + 0.3080x^2 \quad \text{(S9)}$$

where $x = \sqrt{m}$ NaF, is similarly approximated as $\sqrt{I}$.

3M KCl Solution. The activity coefficient of 3M KCl was obtained from published data at 25 ^{o}C to be 0.5690 (Robinson and Stokes, 1965; Table 11, Appendix 8.10), to give an activity for 3M KCl of 1707 mM.

Data Tables

Table S1. Sample table of ion activities for the NaCl dilution experiments

Solution	Ion Conc. (mM)	I (M)	$\sqrt{I}$ ($\sqrt{M}$)	(γ)	a (mM)	$HEPES^-$ (C)	$HEPES^-$ (a)
1.0 Na_o	149.3	0.1500	0.3873	0.7511	112.1	4.3	3.2
0.5 Na_o	79.3	0.0800	0.2828	0.7912	62.7	4.3	3.4
0.25 Na_o	41.7	0.0425	0.2062	0.8322	34.7	4.2	3.5
1.0 Cl_o	145.0	0.1500	0.3873	0.7511	108.9	4.3	3.2
0.5 Cl_o	75.0	0.0800	0.2828	0.7912	59.3	4.3	3.4
0.25 Cl_o	37.5	0.0425	0.2062	0.8322	31.2	4.2	3.5

NaOH concentrations added were 4.3, 4.3 and 4.2 mM for the 1.0 NaCl, 0.5 NaCl and 0.25 NaCl solutions respectively. 136 mM and 189 mM sucrose were added to the 0.5 NaCl and 0.25 NaCl solutions respectively to keep them approximately isoosmotic.

Note that for the recent NaCl biionic experiments, 4.5 mM NaOH needed to be added during the 1.0 NaCl solution buffering, so that an additional 4.5 mM Na^+ ions were allowed for to give a Na^+ concentration of 149.5 mM and activity of 112.3, and a $HEPES^-$ concentration of 4.5 and activity of 3.4.

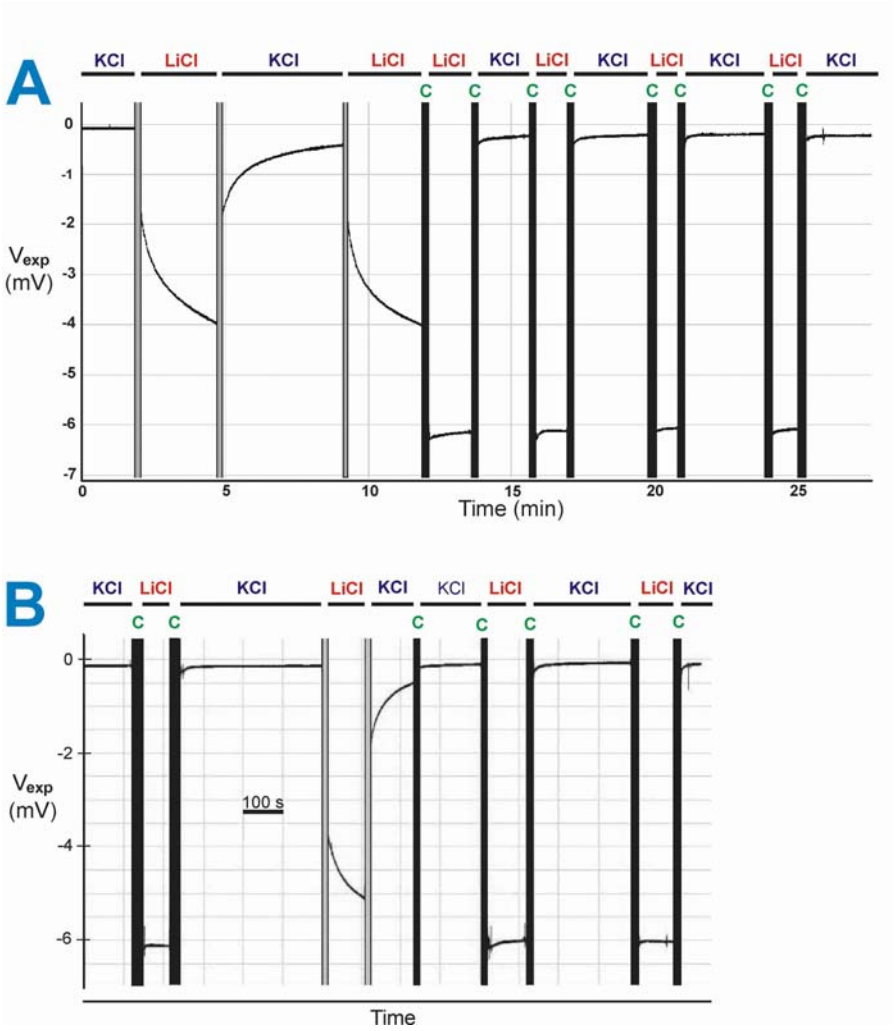

Fig. S2. *Two experimental records to illustrate the necessity of cutting off the tip of the 3M KCl salt-bridge whenever it is transferred to a new solution with different composition (or concentration). The records show the voltage potentials measured between two agar bridge electrodes, a ~150 mM KCl salt-bridge (initially equilibrated with the 145 mM KCl solution) and a 3M KCl reference salt-bridge, both placed in a control (1.0 KCl with 145 mM KCl) or test (1.0 LiCl with 145 mM LiCl) solution as indicated (see setup in Fig. 1 in main paper). The solid bar above each of the traces indicates when the test solution was changed from the 145 mM KCl beaker (KCl) to the 145 mM LiCl beaker (LiCl). The resultant shifts in these junction potentials shown represents the shifts in the sum of the LJPs at the two salt-bridge interfaces. The grey vertical bars on the trace indicate the time during which the solution changeover takes place when the 3M KCl salt-bridges is not cut, and the black vertical bars (and green 'C' above) indicate the time during the solution changeover when the end of the 3M KCl salt-bridge is cut off by at least 6 mm before just before the solution change. In Panel A, the salt-bridges had equilibrated for about 2 hours in the standard 145 mM KCl solution, which allowed the end of the 3M KCl salt-bridge to be replaced in large part by the 145 mM KCl solution. Solution changes then resulted in slow transient responses well below the value expected with a fresh 3M KCl salt-bridge. As soon as that salt-bridge is cut off (this first time by about 2 cm) and the salt-bridges transferred to the LiCl solution, the potential immediately jumps to the maximum value. Subsequent solution changes with a freshly-cut 3M KCl salt-bridge also rapidly jump between the maximum test and control values, as can be clearly seen. Panel B shows a separate experiment illustrating that even a short 6 min equilibration in the KCl solution results in truncated slow transient responses when the solution is changed without the 3M KCl bridge being cut.*

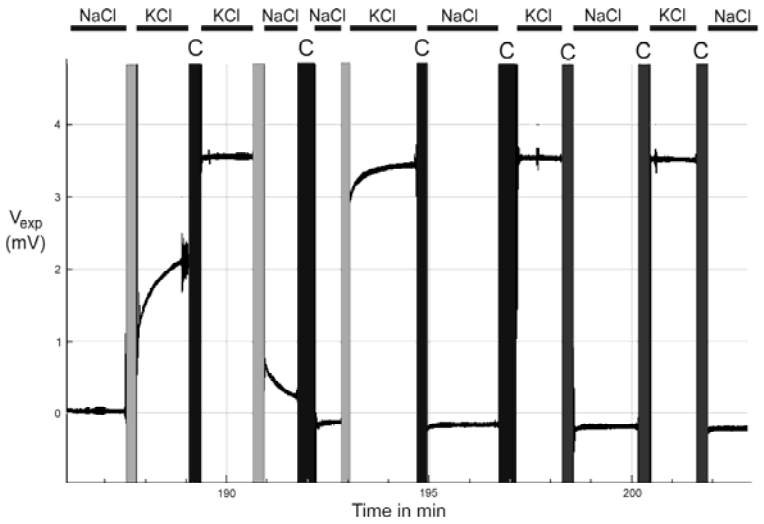

Fig. S3. *The chart record of an experiment in which the freshly-cut tip of a 3M KCl salt-bridge was initially left in the 145 mM NaCl control solution for 120 min to allow the salt-bridge composition to equilibrate with that of the control solution. The bath solution was then changed to 145 mM KCl (as depicted in the horizontal bar above the charts) to record a shift in V_{LJ}, with the salt-bridge not being cut for that solution change (as depicted by a gray vertical bar). Other solution changes and/or salt-bridge cuts are shown by the vertical black bars with a 'C' above them, to indicate the cutting of the end of the 3M KCl salt-bridge by 10 mm (for the first 3 cuts) and then 8-10 mm cuts for the remainder. The first 3 salt-bridge cuts were 10 mm in length and the remainder between 8-10 mm. The figure indicates that after three 10 mm cuts off the end of the salt-bridge, the shift in V_{exp} had reached a maximum value and was no longer transient in time course.*

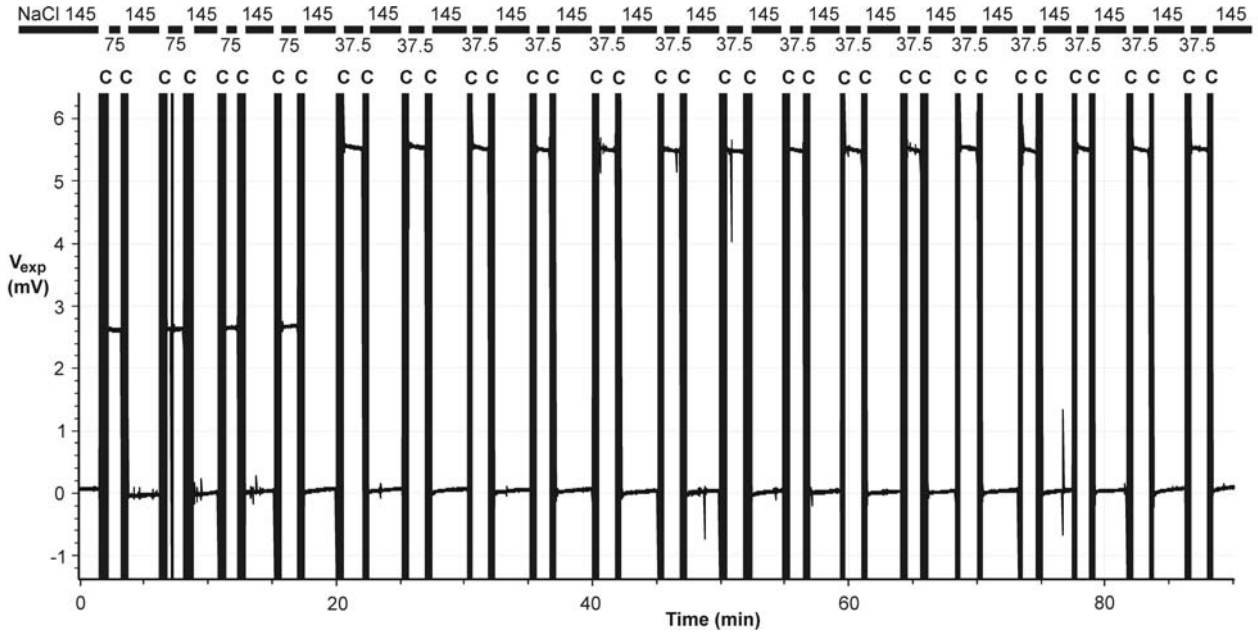

Fig. S4. *Another example of the consistent and rapid rectangular shifts in liquid junction potentials measured for solution dilutions, in this case from 1.0 NaCl to 0.5 NaCl (145 mM to 75 mM NaCl; the first four solution changes) and from 1.0 NaCl to 0.25 NaCl (145 mM to 37.5 mM NaCl; the remainder) at 22°C. See Fig. 1 (main paper) for experimental setup, and* ***Solutions*** *section for full details of solution compositions. Again the LJPs are measured as the difference between a 150 mM NaCl agar salt-bridge (initially equilibrated with a 1.0 NaCl solution) and a 3M KCl reference salt-bridge, when the 3M KCl salt-bridge tip is cut off just prior to every solution transfer. The black vertical bars (and 'C's) indicate the period during which the solution is changed and the tip of the 3M KCl reference salt-bridge was cut, thereby having a fresh 3M KCl interface in contact with the new solution.*

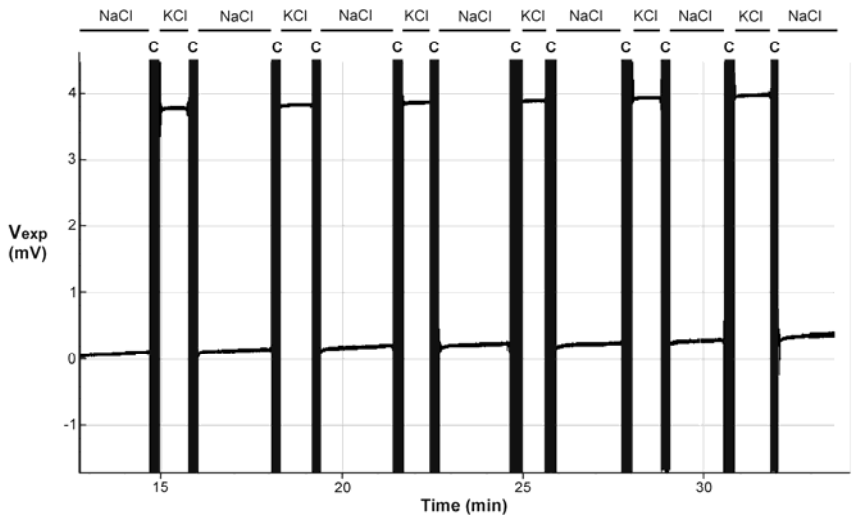

Fig. S5. *An example of the consistent and rapid shifts in liquid junction potentials measured between NaCl and KCl biionic solutions [1.0 NaCl (with 145 mM NaCl) and 1.0 KCl (with 145 mM KCl); at 22°C; see Fig. 1 (main paper) and* ***Solutions*** *section for full details of solution compositions] as the difference between a 150 mM NaCl agar salt-bridge (initially equilibrated with a 1.0 NaCl solution) and a 3M KCl reference salt-bridge, when the 3M KCl salt-bridge tip is cut off just prior to every solution transfer. The black vertical bars (and bold 'C's) indicate the period during which the solution is changed and the tip of the 3M KCl reference salt-bridge was cut, thereby having a fresh 3M KCl interface in contact with the new solution.*

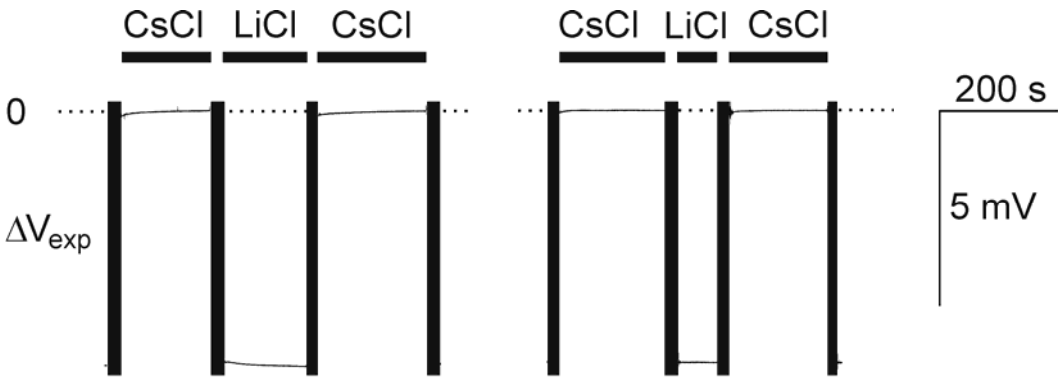

Fig. S6. *An example of the shifts in LJPs measured between CsCl and LiCl biionic solutions [1.0 CsCl (with 145 mM CsCl) and 1.0 LiCl (with 145 mM LiCl); at 22°C; as the difference between a 150 mM CsCl agar salt-bridge (initially equilibrated with a 1.0 CsCl solution) and a 3M KCl reference salt-bridge, when the 3M KCl salt-bridge tip is cut off just prior to every solution transfer (with the black vertical bars indicating the solution transfers when the 3M KCl salt-bridge is cut, as in data shown in Figs S2-S5). However, notice that when the time duration in the LiCl test solution is closer to that in the CsCl control solution (left 3 changes), there is a small initial transient component to the* ΔV_{exp} *shifts, but that when the test solution duration is relatively much shorter, the initial transient components are reduced (right 3 changes).*

Table S2. The limiting equivalent conductivities (Λ^0) of Li^+, Na^+, Cs^+ and Cl^- ions at various temperatures. The published values at 15, 18, 25 and 35 ^oC were obtained from Appendix 6.2 of Robinson and Stokes (1965). The published data at 15, 25 and 35 ^oC are reliable to within the last figure given and the 18 ^oC values to 2 or 3 units in the last figure given. The other asterisked values at 20 and 22 ^oC were fitted (using Sigma Plot 9.0) from quadratic polynomial fits to the published values at all 4 temperatures in the case of Li^+, Na^+, K^+ and Cl^- and to the 15, 25 and 35 ^oC values for Cs^+, though the 18 ^oC value did happen to be close to the fit.

Temp. \ ion (X)	Li^+	Na^+	K^+	Cs^+	Cl^-
15 ^oC	30.2	39.7	59.6	63.1	61.4
18 ^oC	32.8	42.8	63.9	67	66.0
20 ^oC*	*34.35**	*44.81**	*66.53**	*70.05**	*68.84**
21 ^oC*	*35.19**	*45.85**	*67.92**	*71.46**	*70.34**
22 ^oC*	*36.04**	*46.91**	*69.32**	*72.89**	*71.85**
25 ^oC	38.6	50.10	73.50	77.2	76.35
35 ^oC	48.0	61.5	88.2	92.1	92.2

*These values were fitted to an equation in the form ($y = y0 + at + bt^2$, where t is the temp in ^oC, y is the $\Lambda^0(t)$ used to fit them and y0, a and b are the fitting parameters, are as follows:
Li^+: y0=19.444; a=0.65114; b=0.004698; Na^+: y0=25.961; a=0.8451; b=0.004861;
K^+: y0=40.2143; a=1.2428; b=0.003651; Cs^+: y0=43.450; a=1.250; b=0.0040;
Cl^-: y0=40.6275; a=1.3276; b=0.004158.

Possible effect of electric field on Cs^+ mobility

It should be noted that a molecular dynamics study of alkali cation mobilities by Lee and Rasaiah (1994) at infinite dilution indicated that the hydrated water molecules around the alkali cations are bound in inverse proportion to their ionic radii, so that the smallest ion , Li^+ (bare ionic radius 0.068 nm), has **a** primary solvation shell of water molecules 'stuck to it and moving with it as an entity' with a residence time of about 190 ps or longer, behaving as in the classic solventberg model (see Appendix A in Sugiharto et al., 2008). For Na^+ (radius 0.097 nm) this residence time reduces to about 35 ps, whereas for the large Cs^+ ion (radius 0.167 nm) the water molecules are only loosely bound and the residence time is only about 8-11 ps. In addition, Table III in Lee and Rasaiah (1994) suggest**s** that there is a 4% decrease in the number of water molecules coordinated by Cs^+ in the presence of an extremely large electric field compared to in its complete absence, in contrast to the situation**s** for Li^+, Na^+ and K^+. If this is correct, this would seem to be compatible with a reduced u_{Cs} even in the presence of a smaller but still substantial (e.g., 12 V/cm) applied electric field, as used in the measurement of limiting equivalent conductivity. Hence, the loosely bound hydration shell is more likely to be stripped away from the ion than it would be in a much smaller or non-existent electric field, such as might occur under biionic or dilution concentration gradients. If u_{Cs}/u_K at 22 ^oC is reduced from 1.049 to about 1.040 for both CsCl biionic and dilution data, the difference between measured and predicted ΔV_{LJ}s would be reduced to within the expected ± 0.1 mV for CsCl:LiCl and CsCl:NaCl and 0.1 mV outside it for CsCl:KCl bionics and brought into exact agreement for 0.5 and 0.25 CsCl dilutions.

Calculations of concentration profiles of test solute and KCl in the '3M' KCl salt bridge due to KCl and solute diffusion between it and the bath solution (see Fig. 5 in main paper)

From Eqs. 6 and 7 in the main accompanying paper (Barry et al., 2012), and the appropriate diffusion coefficients, we can calculate the changes in concentration profiles of test solute and "3M" KCl in the salt-bridge with time. These changes for NaCl as a test solute after a cut salt-bridge has been in control solution for various conditioning times are given in Table S3 and shown in Fig. 5 of the main paper. The distance scale has been expanded in Fig. S7 for a conditioning time of 20 min (1200 sec) to more readily show the concentration changes over shorter distances for such a conditioning time. For example, in such a case at 20°C, the concentration of the NaCl test solution will have risen to 56% of its bath solution 1 mm in from the end of the salt-bridge, and the KCl solution will have dropped to about 39% of its 3M concentration at that same distance. However, at 5 mm from the end of the salt-bridge, the NaCl concentration will be only 0.3% of its bath concentration and the KCl concentration will have only dropped to 98.9% of its original 3M concentration.

Table S3. Relative concentrations at different distances from the end of a 3M KCl salt-bridge placed in a large volume of test solute with concentration C_{s0}, as a result of the diffusion of test solute into, and KCl out of, the salt bridge. C_{K0} is the initial KCl concentration in the freshly-cut 3M KCl salt-bridge at $t = 0$, and C_K and C_s are the subsequent concentrations of KCl and the test solute within that salt-bridge, respectively, at a later time, t. The values were calculated from Eqs. 5 and 6 in the accompanying paper. Diffusion coefficients were at 25°C and corrected for 4% agar in the 3M KCl salt-bridge (See also Fig. 5 in the main paper).

Time t (min)	Rel concs.	Distances in mm from end of 3M KCl salt bridge					
		0.1	1.0	5.0	10.0	20.0	30.0
5 min	C_s/C_{s0}	0.911	0.266	0.000	0.000	0.000	0.000
	C_K/C_{K0}	0.077	0.664	1.000	1.000	1.000	1.000
20 min	C_s/C_{s0}	0.956	0.578	0.005	0.000	0.000	0.000
	C_K/C_{K0}	0.038	0.370	0.984	1.000	1.000	1.000
120 min	C_s/C_{s0}	0.994	0.943	0.720	0.473	0.151	0.031
	C_K/C_{K0}	0.005	0.050	0.244	0.466	0.786	0.938

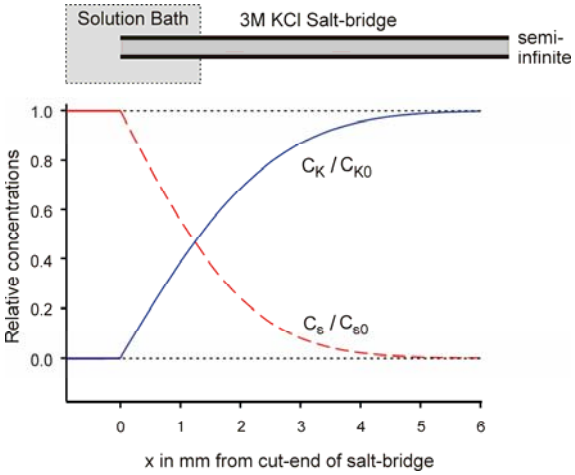

Fig. S7. *A schematic diagram to indicate the relative concentration changes at the tip of an effectively semi-infinite 3M KCl salt bridge with the cut-end placed in an NaCl salt bath. It differs from Fig. 5 (main paper) in that only the curves for a conditioning time in NaCl of 20 min are shown and in that the x axis has been expanded to more readily show the large relative concentration changes within 6 mm from the cut-end of the salt bridge over this time.*

Additional dilution experiments in simple NaCl solutions

Table S4 shows the results of some additional dilution experiments to measure LJPs for simple NaCl solutions without the addition of solutes included in the main paper measurements to represent those used in typical physiological experiments – namely, sucrose to compensate for different solution osmolalities in dilution measurements, glucose and pH buffer (e.g., HEPES and NaOH). The first two rows (150:300 NaCl) and (150:75 NaCl) can be used compare the results for similar concentration gradients, to test whether different absolute NaCl concentrations affect the agreement between measured and predicted LJPs. The second two rows (150:75 NaCl) and (150:37.5) can be used to compare the agreement between measured and predicted values in these simple NaCl solutions with the agreement between measured and predicted NaCl values in the physiologically equivalent '0.5 NaCl' and '0.25 NaCl' dilutions in Table 2 in the main paper.

Table S4: Experimental measurements of liquid junction potentials (ΔV_{LJ}^{m}) in mV at 22 ^{o}C for three simple NaCl solutions, with no added sucrose, glucose or pH buffer, and with concentrations in mM.

Control NaCl	Test NaCl	$-\Delta V_{exp}$	Using activities				n
			ΔV_{3M}	ΔV_{LJ}^{m}	ΔV_{LJ}^{p}		
150	300.0	+2.8 ± 0.01	+0.7	+3.5	+3.4		7
150	75.0	-2.9 ± 0.01	-0.6	-3.5	-3.4		6
150	37.5	-5.9 ± 0.01	-1.1	-7.0	-6.8		7

As indicated' just the calculations using ion activities are shown; m refers to measured values and p to predicted ones. All calculations used converted molality values rather than molarities, and calculation rounding errors are to within ±0.1 mV.

The results shown in the first two rows are consistent with there not being any significant (non-electrical) cross-coupling effects between the Na^+ and Cl^- ions at different absolute concentrations. The results shown in the last two rows indicate that the concentrations of sucrose used did not significantly affect the agreement between measured and predicted LJPs for NaCl dilutions and hence that such concentrations of sucrose do not appreciably affect the magnitudes of the LJPs.

Appendix S1: The relationship between generalized relative ionic mobility and limiting equivalent conductivity

by Peter H. Barry

Firstly, it should be noted that the relative mobility of an ion, u, required for calculating liquid junction potentials (as listed in the tables of mobilities in published sources and required in *JPCalc* calculations) represents the generalised (or absolute) mobility of an ion relative to K^+. For example, if u_X, is the relative mobility for ion X, with respect to K^+, it will be given by:

$$u_X = u^*_X / u^*_K \qquad \text{(S10)}$$

where u^*_X and u^*_K represent the absolute values of the generalised mobilities of ions X and K^+ respectively. The units of the relative mobility for ion X, u_X, are (of course) dimensionless.

The following discussion indicates how the generalised mobilities of ions are in turn related to their limiting equivalent conductivities.

Since the velocity of an ion in solution, v, is related to the generalised (absolute) mobility, u^*, and the generalised force, F_x, acting on it, then:

$$v = u^* F_x \tag{S11}$$

The force may be in Newtons/mole or Newtons, depending on whether it is the force acting on a mole of ions or on a single ion (and whichever is chosen will affect the units of u^*). The above generalised mobility is what is required for electrodiffusion flux equations, and would normally be that required for a force acting on a mole of ions.

In contrast, electrochemists, when measuring conductivity, use another definition of mobility, which may be defined as u', the electrical mobility, sometimes also called the 'conventional' mobility (Bockris and Reddy (1973); pp. 369-373), since they measure the mobility as the velocity/ electric field, E (e.g., in volts/m) as:

$$v = u' E \tag{S12}$$

Since the actual force referred to in Eq S11 is zFE, we also have $v = u^*|z|FE$, where $|z|$ is the magnitude of the valency and F is the Faraday. Hence we have $u' E = u^*|z|FE$ *, and:*

$$u^* = u'/|z|F \tag{S13}$$

We wish to know the relationship between generalised (absolute) mobility and the limiting equivalent conductivity, Λ^0 (the conductivity of an electrolyte solution per equivalent, in the limit as the concentration goes to zero). Now Λ^0 makes allowance for the additional charge of polyvalent ions, so that:

$$u' = \Lambda^0 /F \tag{S14}$$

[cp. equations 4.156 - 4.160 in Bockris and Reddy (1973; p.373) for equivalent conductivity (Λ) and molar conductivity (Λ_m), where $\Lambda = \Lambda_m/|z|$; Note that there is an error in sign of the anion subscript in Eq. 4.160].

Hence, from the two equations above, the generalised mobility, u^*, and Λ^0 will be related by:

$$u^* = \Lambda^0 / (|z|F^2) \tag{S15}$$

{cf. the equation for the generalized mobility, u, of a single ion, rather than a mole of ions, u^*, which is given by $u = N\Lambda^0 / (|z|F^2)$, where N is Avogadro's number (e.g., Eq. A4 in Sugiharto et al., 2008)}. Hence, the relative mobility of ion X of valency z is given by:

$$u_X = \Lambda^0_X / (|z| \cdot \Lambda^0_K) \tag{S16}$$

since, for K^+, $|z| = 1$ and both limiting equivalent conductivities were measured at the same temperature.

For a monovalent ion Y, its relative mobility will simply be given by:

$$u_Y = \Lambda^0_Y / \Lambda^0_K \tag{S17}$$

where Λ^0_Y is the limiting equivalent conductivity of Y at the same temperature as for Λ^0_K , normally 25 ^oC.

For reference, Λ^0_K = 73.50 S.cm^2.equiv^{-1} at 25 ^oC (Robinson and Stokes, 1965).

Appendix S2: The validity of the use of the Henderson equation for calculating LJPs

While the Henderson equation (Henderson, 1907, 1908; MacInnes, 1961) has proved to have been very successful in predicting experimental values of liquid junction potentials (see below), it is not a solution of the Nernst-Planck-Poisson set of electrodiffusion equations. It is based on a thermodynamic derivation of a pseudo steady-state liquid junction potential (LJP) between two liquids obtained by adding up the incremental potentials across a number of small solution layers with slightly varying compositions between two solutions because of the differences in transference (transport) numbers between each of the individual ions. The only assumption made is that each layer represents a mixture of the compositions of the two solutions initially brought into contact (see excellent discussion of the equation derivation in Chapter 13 of MacInnes, 1961). When the appropriate equations are integrated they result in Eqs. (2) and (3) presented in this paper. It should be noted that for two simple situations - a dilution potential between two uni-univalent electrolytes at different concentrations [e.g., NaCl (C_1) : NaCl (C_2); a Type 1 junction] or a biionic potential between two uni-univalent electrolytes at the same concentration but with one of the ions different [e.g., NaCl (C_1) : KCl (C_1); a Type 2 junction] the form of the equations are exactly the same as those of the simple Planck electrodiffusion equation. The latter equation is based on the steady-state solution of the Nernst-Planck electrodiffusion flux equations, with the assumption of a defined (constrained) junction region of known thickness separating the two well-stirred solutions, and the assumption of approximate local concentration "electroneutrality" of the individual local elemental regions across that junction. For a Type 1 junction this gives rise to a linear concentration gradient for both ions. As noted, the Henderson equation has been very successful in predicting experimental values of liquid junction potentials measured with Ag/AgCl (Barry & Diamond, 1970), 3M KCl pipette (Ng & Barry, 1995; Keramidas et al., 1999) and freshly-cut 3M KCl salt-bridge reference electrodes (Sugiharto et al. 2010; Barry et al, 2010) and this present paper, with the last 3 papers using increasingly more refined techniques for accurate measurement of the LJPs.

An important question is how does the Henderson equation compare with rigorous dynamic electro-diffusional theories of liquid junction potentials? As Dickinson et al. (2010) reasonably point out, for typical liquid junction potential situations with unconstrained junctions, the junction region will continue to increase in width with time and the magnitude of the slope of the ion concentration profiles will decrease with time. One basic apparent problem with the "steady-state" Henderson and Planck equations is that they assume an approximate local electroneutrality within the liquid junction region and yet clearly the LJP arises from the integration of the electric field across the junction. This electric field is generated by the differential separation of charge between cations and anions arising from the movement of cations and anions with different mobilities (and hence generally different transport numbers) down their electrochemical gradients. Clearly, when the junction region is still small and the charge separation growing, the imbalance between anions and cations over small distances can be substantial and the electric field large. As indicated by Dickinson et al. (2010), this problem was first addressed properly in the 1960-1970s. In 1965, Hafemann used a numerical computer simulation together with the principles of irreversible thermodynamics to calculate the electro-diffusion of each of the ions at a junction of two unconstrained uni-univalent electrolytes (Type 1 junction). By dividing the junction into about 100 planar elements and using an integration formulation of Gauss' law the electric field was calculated in each element generated from a summation of the charge imbalance in the other elements. He showed that for his salt dilution junction example, the LJP rapidly asymptotes to a maximum steady value, with a rise time of about 10^{-9} s, with the steady-state value agreeing with predictions of the

Henderson equation. Hickman (1970) outlined a more general, rigorous approach to this problem, using the Nernst-Planck equations and the Poisson equation (derived from Gauss's law), using perturbation techniques to generate analytical power series expansions, for multiple ionic components and even allowing for incompletely ionized systems. Importantly, he showed that the Henderson equation was the leading term in a series expansion of power terms of a small parameter, with all the other terms becoming insignificant for long times. In 1974, Jackson, refined Hickman's approach for the case of two univalent ions in a dilution liquid junction, to elucidate the underlying physical explanation of what this parameter represents and what is occurring in the LJP over such times. He provided a simple explanation of the paradox of the development of a steady potential and apparent charge electroneutrality. At any point, the charge density decreases to zero with time (t) as t^{-1}, the spread of charge increases as $t^{1/2}$, so the net charge per unit area decreases as $t^{-1/2}$. Since the potential difference is of the order of the product of the electric field (which is proportional to the charge per unit area, which goes as $t^{-1/2}$) and the separation (proportional to $t^{1/2}$ for large times), the potential difference should be constant. This indicated for such a system why the LJP should be time-independent for times greater than about 10^{-9} s (assuming reasonably that the solution boundaries may be considered to be semi-infinite for the times involved), and why the LJP is given by the Henderson equation. Recently, Perram and Styles (2006) used a numerical analysis of the Nernst-Planck-Poisson equations and perturbation theory for the liquid junction potential of a uni-univalent salt gradient (Type 1 junction) across a thick porous membrane (constrained junction) to show that the LJP initially rose rapidly and then also asymptoted to the Henderson equation.

More recently, Compton and colleagues (Dickinson et al., 2010, Ward et al., 2010 and Zhurov et al., 2011) have used a more exact and rigorous Nernst-Planck-Poisson (NPP) finite difference numerical simulation system, together with perturbation analyses, to confirm and extend the basic conclusions of the above earlier studies, and produce a complete quantitative simulation of the dynamic evolution of the liquid junction potential across an unconstrained junction, together with the evolution of the profiles of the ionic concentrations and electric field across the expanding junction region, from the moment the two different semi-infinite solutions first come into contact. Dickinson et al., (2010) in particular determined the evolution of the electric field profiles across the liquid junction for a range of different time durations for both Type 1 dilution junctions (Fig. 6) and Type 2 biionic junctions (Fig. 15). They showed that in both cases, the electric field initially rose very rapidly to a maximum in a 5-50 ns timescale with a very narrow spike profile, before reducing in height and continuing to broaden out with time as in Figs. 6 and 15. With respect to the magnitude of the LJP, they validated the previous asymptotic analyses by Hickman (1970) and Jackson (1974) and showed that the LJP rapidly rises to a maximum steady plateau value [given by $-\Delta\theta_{LJP}$ in Figs. 2 and 11 of Dickinson et al., 2010 for Type 1 (dilution) and Type 2 (biionic) junctions respectively] close to the values predicted by the Henderson equation. In their accompanying online Supporting Information C, Dickinson et al. (2010) also demonstrated strong agreement (within 0.25% in their simulations) with the Henderson equation for the LJP magnitudes ($\Delta\theta_{LJP}$) in the Type 1 junctions for a range of different cation/anion mobilities (Fig 1), with it tending to exact agreement with the Henderson equation for theoretical asymptote perturbation analyses. For Type 2 junctions, Dickinson et al. (2010) found good, but not quite so strong, agreement (within 0.8%) for $\Delta\theta_{LJP}$ for a range of different cation-cation mobilities for Type 2 junctions (Fig 2). In support of these latter results, they showed (Supporting Information H) that the asymptotic analysis of Hickman (1970) for Type 2 junctions required "…a further perturbation involving diffusion coefficients …. to achieve approximate results for this asymptote…" and so was not in exact agreement with the Henderson equation. They indicated that LJP reaches steady value "…at time scales of 10-1000 ns after junction potential formation for typical aqueous systems, by which time the diffuse layer is approximately 10-1000 nm in extent and is continually expanding …" Dickinson et al. (2010).

Ward et al. (2010) in the Compton group used the same approach to investigate Type 3 junctions (A^+X^- || B^+Y^- ; e.g., biionics with no common anion) with a multilayer liquid junction and found there could be greater deviations from the Henderson equation. Nevertheless, for the junction (KNO3 || NaCl), where there were relatively small differences in relative mobilities (1, 0.682, 0.972, 1.039 respectively; proportional to their diffusion coefficients), they calculated a very close agreement with the Henderson equation (with difference < 0.01%) for a calculated LJP of 5.37 mV for that equation. Even for the junction ($Na^+Acetate^-$ || K^+OH^-), where there are substantial differences in relative ion mobilities (0.682, 0.556, 1.0, 2.69 respectively; http://web.med.unsw.edu.au/phbsoft/mobility_listings.htm), they only observed a deviation of 1.55% from their simulated value of 20.4 mV compared to the value of 20.72 mV from the Henderson equation**.** They did indicate that when there was a much more substantial difference between the maximum and minimum relative ionic diffusion coefficients (or relative ion mobilities) the deviation from the Henderson equation could increase further and be more than 8%. They defined a small parameter $\mu = (D'_{max} - D'_{min})/(D'_{max} + D'_{min})$ as in Eq. 3.5 of their paper, where D'_{max} and D'_{min} are the maximum and minimum single ion diffusion coefficients for the four ion species in the junction. Asymptotic analysis (Hickman, 1970) resulted in the first term of an expansion being equal to the Henderson equation (for long times), with a power series of μ terms, and in relatively extreme cases, this could produce very significant deviations from the Henderson equation for Type 3 junctions. They also observed that larger deviations from the Henderson equation occurred when both the cation and anion on one side of the membrane had greater ionic diffusion coefficients, but similar to each other, than those ions on the other side of the junction (Ward et al., 2010). *It should also be appreciated that the above mobility comments are only relevant to the mobilities of the predominant four ion species in the solutions, which were all that were considered in the above cases, and that the inclusion of* ***small concentrations of*** *additional ions, which have either very low or very high mobilities, to solutions with high concentrations of more standard ions will only contribute minimally to the LJP. In addition, for almost all relevant predominant ions in physiological solutions, the range of ion mobility values would be much less than in the above KOH case.*

In summary, these informative theoretical studies on the evolution and underlying mechanisms of LJPs provide validity and a theoretical rationale for the use of the Henderson equation for calculating pseudo 'steady-state' LJPs in the double semi-infinite solution junction described above. In particular, the theoretical analyses by Compton et al. suggest that while Type 1 junctions are expected to give exact asymptotic agreement with the Henderson equation, subtle small differences between experimental LJPs and predictions of the Henderson equation may be expected with Type 2 biionic junctions (e.g., 0.8%), and greater differences with the Type 3 biionic junction (e.g., 1.55%) with greater mobility differences. These papers provide a strong theoretical basis for the validity of the Henderson equation as an approximate asymptotic estimate of the LJP for various types of junctions and indicate where significant deviations from the Henderson could occur.

Furthermore, it should also be noted that for the salt-bridge – solution bath system discussed in this present paper, the interface between a small salt-bridge in contact with a large volume bath, is likely to behave as a constrained boundary, which would tend to hold the composition at that interface close to the bath composition, whereas the salt-bridge (or pipette) would behave as a semi-infinite solution. This would result in a much simpler system than two semi-infinite solutions in contact and it seems most likely that the pseudo steady-state LJP of such a single semi-infinite junction should be even more closely approximated by the Henderson equation, maybe at least halving the above deviations. Such a system could be a worthy subject for a rigorous Nernst-Planck-Poisson analysis.

As Hafeman (1965) points out in his analysis, which is clearly true of all the above theoretical analyses discussed, none of them assumes the presence of any non-electrical cross interaction between different ion fluxes or effects due to solvent convection. Such effects have been modeled in considerable detail by Mori et al. (2011) using principles of irreversible thermodynamics to

simulate electro-diffusion and osmotic water flow across cell membranes and tissues. With respect to the differences in osmotic concentrations between the agar salt-bridges and bath solutions, it might be thought that this could give rise to some solvent flow between them. However, since the agar salt-bridges are an open porous matrix with less than a 10% drop in diffusion coefficient, it would be expected that the reflection coefficient for sucrose would be zero and that there would be no solvent flow in or out of the salt-bridges. The predicted lack of osmotic effects for salt-bridges was confirmed when dilution LJPs were measured in the absence of any osmotic sucrose compensation for NaCl solutions with dilutions to 50% and 25% concentrations, where there was also excellent agreement between measured and calculated LJPs using the Henderson equation (see ESM Table S4 in the Electronic Supplementary Material). Similarly, if cross-coupling effects were significant in such LJPs, there might be expected to be a difference between two-fold gradients at different absolute salt concentrations. However, the measured values for a simple NaCl salt gradient of 150:300 and for a 150:75 gradient were equal in magnitude, but with reversed sign (ESM Table S4), consistent with no convective effects. In addition, while there are small effects of sucrose on Ag/AgCl electrode potentials (e.g., of about 0.3 mV for 200 mM sucrose; Barry & Diamond, 1970) these are not relevant with the freshly-cut 3M KCl salt-bridge reference system technique used in this paper. However, it is known that sucrose will reduce the dielectric constant of aqueous solutions (e.g., a decrease of ~2.5% at 25 ^{o}C; Akode et al., 2004), which would tend to slightly increase the activity coefficients of all the ions in solution. Since the contribution of activity coefficients in LJPs is small anyway (see Table 2), this seems unlikely to be very significant. Another possible effect of the sucrose is on the hydration of the ions. From molecular dynamics and potential of mean force calculations on aqueous sucrose solutions of an Na-Cl ion pair, Martorana et al. (2000) have estimated that a 60% w/w (~4.4 molal) solution of sucrose will reduce the first hydration shell of Cl^{-} from 3.6 to 2.8 (22% decrease) water molecules and that of Na^{+} from 5.9 to 5.0 (15%), but since this sucrose concentration is about 22 times greater than the sucrose concentrations used in this present paper (~200 mM sucrose), the effect on relative mobilities is likely to be very small. This is shown by the LJP measurements and calculations in the presence (~190 mM sucrose) and absence of sucrose for the 0.25 NaCl dilutions (in Tables 2 and S4). These results indicate that the concentrations of sucrose used did not significantly affect the agreement between measured and predicted LJPs for NaCl dilutions and hence that such concentrations of sucrose do not appreciably affect the magnitudes of the LJPs.

However, with a pipette reference electrode, instead of a salt-bridge, in contact with a bath, if the solution in the pipette were free-flowing under a hydrostatic gradient, to minimize history-dependent effects, the resultant volume flow may have a convective effect on the magnitude of the LJP.

Appendix S3 Measurement and calculation of LJPs when ion mobilities are not known

If the mobilities of one or more of the major ions in a solution are not known accurately, then the LJP can be directly measured, but for an accurate LJP value there still needs to be a correction for the ΔV_{3M} contribution to the LJP? But how can this correction be calculated without values for all the ion mobilities? First of all, as Tables 2 and 3 in the main paper indicate, the contribution of the ΔV_{3M} term is a second order effect (e.g., there is only a 0.2 mV difference in the ΔV_{3M} term between the 0.25 dilutions of NaCl and LiCl) and only a very rough estimate of the non-KCl ion mobilities is needed (either from known mobilities of ions of a similar size and properties) in order to estimate the .ΔV_{3M} contribution to the LJP (see further discussion in ESM). It should be noted from the above tables that ΔV_{3M} is generally only a relatively small fraction of the measured LJP, except when the ion mobilities are very similar, in which case both the LJP and ΔV_{3M} are very small anyway.

If the unknown ion is one of the major ones, then trial values of that unknown ion can be iteratively tried and the corrected measured LJP value (e.g., ΔV_{LJ}^{ma} in Tables 2 and 3 or ΔV_{LJ}^{m} in

Table S4) compared with the calculated value (e.g., ΔV_{LJ}^{pa} in Tables 2 and 3 or ΔV_{LJ}^{p} in Table S4) to minimize the divergence between the two values. Indeed, LJP measurements with the above technique could be used in simple uni-univalent salt dilution measurements, for an ion with unknown mobility in combination with a counterion of known mobility, to at least estimate the mobility of the first ion, without having to do limiting equivalent conductivity measurements.

References

Barry PH, Lewis TM, Moorhouse AJ (2012) An optimised 3M KCl salt-bridge technique used to measure and validate theoretical liquid junction potential values in patch-clamping and electrophysiology, Eur Biophys J (submitted)

Barry PH, Sugiharto S, Lewis TM, Moorhouse AJ (2010) Further analysis of counterion permeation through anion-selective glycine receptor channels. Channels 4:142-149

Bockris JO'M, Reddy AKN (1973). Modern Electrochemistry, Vol 1, Plenum Press, New York

Cui R-F, Hu M-C, Jin L-H, Li S-N, Jiang Y-C, Xia S-P (2007). Activity coefficients of rubidium chloride and cesium chloride in methanol-water mixtures and a comparative study of Pitzer and Pitzer-Simonson-Clegg models (298.15 K). Fluid Phase Equilibr 251:137-144.

Dickinson EJF, Freitag L, Compton RG (2010) Dynamic theory of liquid junction potentials. J Phys Chem 114:187-197

Hafemann DR (1965) Charge separation in liquid junctions. J Phys Chem 69:4226-4231

Henderson P (1907) Zur thermodynamic der Flüssigkeitsketten. Z Phys Chem 59:118-127

Henderson P (1908) Zur thermodynamic der Flüssigkeitsketten. Z Phys Chem 63:325-345

Hickman HJ (1970) The liquid junction potential - the free solution junction. Chem Eng Sci 25:381-398

Ives DJG, Janz GJ (1961). Reference Electrodes. Academic Press, New York

Jackson JL (1974) Charge neutrality in electrolyte solutions and the liquid junction potential. J Phys Chem 78:2060-2064

Lee HL, Rasaiah JC (1994). Molecular dynamics simulation of ionic mobility. I. Alkali metal cations in water at 25 ^{o}C. J Chem Phys 101: 6964-6974.

MacInnes DA (1961) The Principles of Electrochemistry. Dover Publications, Inc. New York

Mori Y, Liu C, Eisenberg RS (2011) A model of electrodiffusion and osmotic water flow and its energetic structure. Physica D 240: 1835-1852

Perram JW, Stiles PJ (2006) On the nature of liquid junction and membrane potentials. Phys Chem Chem Phys 8:4200-4213

Robinson RA, Stokes RH (1965) Electrolyte Solutions, 2nd Ed. Revised. Butterworths. London.

Sugiharto S, Lewis TM, Moorhouse AJ, Schofield PR, Barry PH (2008). Anion-cation permeability correlates with hydrated counter-ion size in glycine receptor channels. Biophys J 95:4698-4715.

Sugiharto S, Carland JE, Lewis TM, Moorhouse AJ, Barry PH (2010). External divalent cations increase anion-cation permeability ratio in glycine receptor channels. Pflügers Arch 460: 131-152.

Ward KR, Dickinson EJF, Compton RG (2010) Dynamic theory of type 3 liquid junction potentials: formation of multilayer liquid junctions. J. Phys Chem B 114: 4521–4528

Zhurov K, Dickinson EJF, Compton RG (2011) Dynamics of ion transfer potentials at liquid-liquid interfaces: the case of multiple species. 115: 12429–12440